

## 1 Authors

2 Brittany A. Petros<sup>1,2,3,4,\*</sup>, Jillian S. Paull<sup>1,4,\*†</sup>, Christopher H. Tomkins-Tinch<sup>1,5,\*†</sup>, Bryn C.  
3 Loftness<sup>1,6,7,8,\*†</sup>, Katherine C. DeRuff<sup>1</sup>, Parvathy Nair<sup>1</sup>, Gabrielle L. Gionet<sup>1</sup>, Aaron Benz<sup>9</sup>, Taylor  
4 Brock-Fisher<sup>1</sup>, Michael Hughes<sup>10</sup>, Leonid Yurkovetskiy<sup>11</sup>, Shandukani Mulaudzi<sup>12</sup>, Emma  
5 Leenerman<sup>10</sup>, Thomas Nyalile<sup>11</sup>, Gage K. Moreno<sup>1</sup>, Ivan Specht<sup>1</sup>, Kian Sani<sup>1</sup>, Gordon Adams<sup>1</sup>,  
6 Simone V. Babet<sup>13</sup>, Emily Baron<sup>14</sup>, Jesse T. Blank<sup>10</sup>, Chloe Boehm<sup>1,15</sup>, Yolanda Botti-Lodovico<sup>1</sup>,  
7 Jeremy Brown<sup>10</sup>, Adam R. Buisker<sup>10</sup>, Timothy Burcham<sup>16</sup>, Lily Chylek<sup>1</sup>, Paul Cronan<sup>16</sup>, Valentine  
8 Desreumaux<sup>13</sup>, Megan Doss<sup>17</sup>, Belinda Flynn<sup>10</sup>, Adrienne Gladden-Young<sup>1</sup>, Olivia Glennon<sup>16</sup>,  
9 Hunter D. Harmon<sup>10</sup>, Thomas V. Hook<sup>13</sup>, Anton Kary<sup>18</sup>, Clay King<sup>19</sup>, Christine Loreth<sup>1</sup>, Libby  
10 Marrs<sup>16</sup>, Kyle J. McQuade<sup>18</sup>, Thorsen T. Milton<sup>13</sup>, Jada M. Mulford<sup>18</sup>, Kyle Oba<sup>16</sup>, Leah  
11 Pearlman<sup>1</sup>, Mark Schifferli<sup>16</sup>, Madelyn J. Schmidt<sup>10</sup>, Grace M. Tandus<sup>13</sup>, Andy Tyler<sup>10</sup>, Megan E.  
12 Vodzak<sup>1</sup>, Kelly Krohn Bevill<sup>6</sup>, Andres Colubri<sup>1,20</sup>, Bronwyn L. MacInnis<sup>1</sup>, A. Zeynep Ozsoy<sup>18</sup>, Eric  
13 Parrie<sup>14</sup>, Kari Sholtes<sup>6,13</sup>, Katherine J. Siddle<sup>1,5</sup>, Ben Fry<sup>16,‡</sup>, Jeremy Luban<sup>1,11,21,22,‡</sup>, Daniel J.  
14 Park<sup>1,‡</sup>, John Marshall<sup>10,‡</sup>, Amy Bronson<sup>23,‡</sup>, Stephen F. Schaffner<sup>1,‡</sup>, Pardis C. Sabeti<sup>1,5,22,24,25,‡</sup>

15  
16 <sup>1</sup>Broad Institute of MIT and Harvard, Cambridge, MA, 02142, USA. <sup>2</sup>Harvard-MIT Program in Health Sciences and  
17 Technology, Cambridge, MA, 02139, USA. <sup>3</sup>Harvard/MIT MD-PhD Program, Boston, MA, 02115, USA. <sup>4</sup>Systems,  
18 Synthetic, and Quantitative Biology PhD Program, Department of Systems Biology, Harvard Medical School, Boston,  
19 MA, 02115, USA. <sup>5</sup>Department of Organismic and Evolutionary Biology, Harvard University, Cambridge, MA, 02138,  
20 USA. <sup>6</sup>Department of Computer Science and Engineering, Colorado Mesa University, Grand Junction, CO, 81501,  
21 USA. <sup>7</sup>Complex Systems and Data Science PhD Program, University of Vermont, Burlington, VT, 05405, USA.  
22 <sup>8</sup>Vermont Complex Systems Center, University of Vermont, Burlington, VT, 05405, USA. <sup>9</sup>Degree Analytics, Inc.,  
23 1905 Kramer Lane Suite A100, Austin, TX, 78758, USA. <sup>10</sup>Colorado Mesa University, Grand Junction, CO, 81501,  
24 USA. <sup>11</sup>Program in Molecular Medicine, University of Massachusetts Chan Medical School, Worcester, MA, 01655,  
25 USA. <sup>12</sup>Harvard Program in Bioinformatics and Integrative Genomics, Harvard Medical School, Boston, MA, 02115,  
26 USA. <sup>13</sup>Department of Civil, Environmental, and Architectural Engineering, University of Colorado, Boulder, CO,  
27 80309, USA. <sup>14</sup>COVIDCheck Colorado, LLC., Denver, CO, 80202, USA. <sup>15</sup>Princeton University Molecular Biology  
28 Department, Princeton, NJ, 08544, USA. <sup>16</sup>Fathom Information Design, Boston, MA, 02114, USA. <sup>17</sup>Warrior  
29 Diagnostics, Inc., Loveland, CO, 80538, USA. <sup>18</sup>Department of Biological Sciences, Colorado Mesa University, Grand  
30 Junction, CO, 81501, USA. <sup>19</sup>Department of Mathematics and Statistics, Colorado Mesa University, Grand Junction,  
31 CO, 81501, USA. <sup>20</sup>University of Massachusetts Medical School, Worcester, MA, 01655, USA. <sup>21</sup>Biochemistry and  
32 Molecular Pharmacology, University of Massachusetts Medical School, Worcester, MA, 01655, USA.  
33 <sup>22</sup>Massachusetts Consortium on Pathogen Readiness, Boston, MA, 02115, USA. <sup>23</sup>Physician Assistant Program,  
34 Department of Kinesiology, Colorado Mesa University, Grand Junction, CO, 81501, USA. <sup>24</sup>Department of  
35 Epidemiology, Harvard T.H. Chan School of Public Health, Boston, MA, 02115, USA. <sup>25</sup>Howard Hughes Medical  
36 Institute, Chevy Chase, MD, 20815, USA.

37  
38 \* These authors contributed equally.

39 † corresponding authors: [tomkinsc@broadinstitute.org](mailto:tomkinsc@broadinstitute.org) (lead contact); [jpaull@broadinstitute.org](mailto:jpaull@broadinstitute.org) (wastewater);  
40 [bloftnes@broadinstitute.org](mailto:bloftnes@broadinstitute.org) (wifi)

41 ‡ These authors jointly supervised this work.

## 42 Title

43 **Multimodal surveillance of SARS-CoV-2 at a university enables development of a robust**  
44 **outbreak response framework**

## 45 Abstract

46 Universities are particularly vulnerable to infectious disease outbreaks and are also ideal  
47 environments to study transmission dynamics and evaluate mitigation and surveillance  
48 measures when outbreaks occur. Here, we introduce a SARS-CoV-2 surveillance and response  
49 framework based on high-resolution, multimodal data collected during the 2020-2021 academic  
50 year at Colorado Mesa University. We analyzed epidemiological and sociobehavioral data  
51 (demographics, contact tracing, and wifi-based co-location data) alongside pathogen  
52 surveillance data (wastewater, random, and reflexive diagnostic testing; and viral genomic  
53 sequencing of wastewater and clinical specimens) to characterize outbreak dynamics and  
54 inform policy decisions. We quantified group attributes that increased disease risk, and  
55 highlighted parallels between traditional and wifi-based contact tracing. We additionally used  
56 clinical and environmental viral sequencing to identify cryptic transmission, cluster  
57 overdispersion, and novel lineages or mutations. Ultimately, we used distinct data types to  
58 identify information that may help shape institutional policy and to develop a model of pathogen  
59 surveillance suitable for the future of outbreak preparedness.

## 60 Intro

61 Infectious disease outbreaks are existential threats to congregate communities; in universities,  
62 in particular, students are susceptible because of close-quarters housing<sup>1,2</sup>, dense social  
63 networks<sup>3-5</sup>, and widespread involvement in sports teams and other student organizations<sup>5,6</sup>.  
64 Students may also be individually vulnerable to infection due to sleep deprivation<sup>7</sup> and poor  
65 hygiene<sup>8</sup>. In addition to their own susceptibility, universities have potential to drive transmission  
66 in surrounding communities<sup>9-11</sup>.

67  
68 At the same time, residential universities are ideal environments for the study of pathogen  
69 transmission and the impact of interventions and surveillance thanks to their semi-insular  
70 character and their role as centers of innovation<sup>12</sup>. In response to SARS-CoV-2 they have  
71 widely employed high-cadence testing<sup>13-15</sup>, vaccination programs<sup>16,17</sup>, strict quarantine of cases  
72 in dedicated facilities<sup>18-21</sup>, and social distancing measures<sup>22-25</sup>. In addition, universities are well-  
73 positioned to test and implement new surveillance methods that can subsequently be applied at  
74 greater scale. For example, they were among the first to implement wastewater surveillance for  
75 SARS-CoV-2<sup>18,26</sup>, institution-wide viral sequencing<sup>21,27</sup>, and contact tracing via wifi network co-  
76 location data<sup>28,29</sup>.

77  
78 In Fall 2020, Colorado Mesa University (CMU) committed to in-person instruction of ~8,000  
79 students for the 2020–2021 academic year, motivated by a desire to avoid amplifying resource  
80 disparities via remote learning. This decision necessitated a rigorous SARS-CoV-2 surveillance  
81 program, balancing public health goals with efficient use of limited resources. Given these  
82 considerations, CMU eschewed mandatory periodic testing of all university community members  
83 in favor of a surveillance program with randomized testing and robust reflexive testing – *i.e.*,  
84 strategic testing of students due to symptoms (reported through the *Scout* web-based tool<sup>30</sup>),  
85 contact with recently diagnosed individuals, or a positive wastewater signal in their residential  
86 dorm.

87  
88 CMU piloted *Lookout*, a tool integrating multiple data types to identify, alert, and test individuals  
89 or groups at increased risk of infection (Figure 1; demo: [https://sentinel.network/lookout-demo-](https://sentinel.network/lookout-demo-campus)  
90 [campus](https://sentinel.network/lookout-demo-campus)). Lookout integrated numerous data types, including clinical diagnostic test results,  
91 student attributes such as residence hall and sports team affiliations, self-reported contacts of  
92 positive individuals, viral genome sequences from diagnostic specimens, and wastewater viral  
93 titers. The interactive dashboard allowed the administration to quickly identify students at risk of  
94 infection and to minimize opportunities for transmission. Here, we explore the utility of  
95 combining these and additional data types (including wifi co-location logs and genome  
96 sequences from wastewater effluent) to design effective disease surveillance systems.

## 97 Results

### 98 1. CMU deployed a comprehensive and effective surveillance program based on a 99 multi-pronged testing approach

100 Over the 2020–2021 academic year, CMU's surveillance program identified 1,113 COVID-19  
101 cases (1,076 students, 37 faculty or staff) through randomized and targeted (*i.e.*, symptomatic  
102 or reflexive) testing. The test positivity rate was 5.1% in Fall 2020 (August 17–November 20)  
103 and 1.5% in Spring 2021 (January 18–April 30) (Figure 2A–C); individuals who tested positive  
104 were moved to an isolation dorm. CMU's randomized testing strategy sampled students non-  
105 uniformly to test more frequently those at greater risk of onward transmission, *i.e.*, on-campus  
106 students and athletes. Consistent with this bias, on-campus students and athletes ultimately  
107 tested positive 1.30 and 2.45 times as frequently as expected given uniform sampling (Appendix  
108 Figure 1C).

109  
110 In addition, CMU's reflexive testing program tested individuals identified by institutional contact  
111 tracing as close contacts. Of the identified positive individuals, 720 (65%) reported close  
112 contacts, enabling subsequent detection of 93 distinct cases (8.4% of the total cases) within a  
113 week of the sentinel case's positive test. These efforts identified plausible transmission links;  
114 among pairs of sequenced cases identified via contact tracing, 79% had closely related  
115 genomes (with a genetic distance of at most two mutations), compared to 10% among  
116 sequenced pairs more generally (Appendix Figure 2A).

117  
118 Frequent wastewater surveillance enhanced reflexive testing efforts, identifying SARS-CoV-2-  
119 positive residence halls whose residents were then randomly selected for follow-up testing. The  
120 effort captured effluent from ~75% (Fall) and ~85% (Spring) of the residential student  
121 population. In response to spikes in viral titer, contributing residence halls were oversampled for  
122 testing; when warranted, up to half of the residents of a hall were tested. The success of this  
123 program is reflected in the close correlation of wastewater viral titer with contemporaneous case  
124 counts (Spearman  $\rho=0.40$ ,  $p<.001$ ; Figure 5AB, Appendix Figure 3).

125  
126 To assess the overall efficacy of CMU's surveillance program, we compared CMU's incidence  
127 rate to that of Mesa County, which had limited testing available at the time. CMU's weekly

128 incidence exceeded county incidence rates and predicted them with a lag time of 3 days  
129 (correlation = 0.73; Appendix Figure 1AB). This is consistent with reports that adequate  
130 university testing can foreshadow community outcomes<sup>12</sup> and highlights the ability of well-  
131 designed university testing programs to serve as bellwethers. As the pandemic's impact on the  
132 surrounding community became clearer, the university sponsored testing for external  
133 community members, both as a public benefit and to limit spread of SARS-CoV-2 into the  
134 campus<sup>31</sup>.

## 135 2. Epidemiological analyses identified student attributes associated with SARS- 136 CoV-2 positivity and support a surveillance paradigm of targeted testing and risk 137 mitigation

138 Here we evaluate risk factors among a wide range of institutionally captured attributes for  
139 individuals who tested positive: role (*i.e.*, student or faculty/staff), sex, class year<sup>32</sup>, test date,  
140 association with a residence hall, and membership in a sports team. Residence halls (Appendix  
141 Table 1) and sports teams (Appendix Table 2) were annotated with features, including  
142 perceived contact risk for sports teams (defined in Appendix Table 3). Our results support a two-  
143 pronged surveillance strategy, in which groups at increased risk are targeted for higher-cadence  
144 testing, while putatively causal factors are mitigated via institutional policies that reduce risk.

145  
146 Besides athletes and on-campus students, whose higher risk of testing positive could reflect  
147 increased sampling, males, freshmen, and juniors also exhibited more cases than expected by  
148 chance (Appendix Figure 1C; Figure 2E; Appendix Table 4). These findings may underscore  
149 risk factors relevant for other universities: for example, a potential commonality between  
150 freshmen and juniors is that many students moved to new living arrangements (on-campus for  
151 freshmen, off-campus for juniors). Future surveillance efforts could target populations  
152 undergoing such transitions, though real-time epidemiology is essential to identify community-  
153 specific risk factors.

154  
155 Looking more closely among sports teams, we identified specific attributes that further predict  
156 disease risk. High-contact sports teams had increased disease risk (Appendix Table 4), with  
157 50% more cases than expected from the risk for athletes as a whole, while low-contact teams  
158 had 47% fewer. Interestingly, risk was not uniform across teams of comparable contact level;  
159 women's basketball had 90% more cases than expected, while men's soccer had 16% fewer,  
160 despite both being high-contact sports (Figure 2D). We found no association between sports  
161 location (*i.e.*, indoor vs. outdoor sports) and case counts, though sports played in both seasons  
162 had higher case incidence than fall or spring sports (Appendix Table 4). These findings are  
163 consistent with a model where individual athletes sporadically contract COVID-19, with an  
164 increased risk of further transmission and thus outbreaks on higher-contact teams or teams with  
165 longer seasons.

166  
167 Because COVID-19 incidence rates varied approximately three-fold from 9.7% to 27% across  
168 residence halls (Appendix Table 1), we conducted linear regression with multiple possible  
169 predictors related to halls to characterize factors that influenced case rates (Appendix Figure  
170 4AB). Two features were significant predictors: percent occupancy (*i.e.*, number of available

171 beds filled) and private (vs. hallway) bathrooms (see Appendix Figure 4C-E for model  
172 validation). We included an indicator variable for fall wastewater tracking to assess whether  
173 reflexive testing biased hall incidence rates; it was dropped as a predictor and thus does not  
174 significantly bias rates.

175  
176 For every increase of 10% in occupancy, our model predicted an increase of 0.015 in incidence,  
177 supporting institutional de-densification measures to limit the transmission risks associated with  
178 denser populations. Strikingly, halls with en-suite or private bathrooms were predicted to have  
179 an incidence 0.059 higher than those with hallway bathrooms (Appendix Figure 4B), consistent  
180 with reports that a majority of SARS-CoV-2 transmissions occur within households (here, within  
181 suites)<sup>33</sup>. Possible explanations include compensatory protective measures (*i.e.*, masking or  
182 social distancing) present in larger bathrooms and the increased hygiene of hallway bathrooms,  
183 which were cleaned by professional staff rather than residents. Importantly, our model does not  
184 account for possible social confounders such as clustering of certain groups (*e.g.*, athletes or  
185 freshmen) within specific residence halls.

### 186 3. Distinct interaction dynamics of positive individuals within wifi proximity dataset 187 reveal potential for incorporation into disease surveillance

188 Here, we explore a dataset of anonymized daily logged connection locations (*i.e.*, access point  
189 and building) for students connected to campus wifi for at least 15 minutes, and describe how  
190 such data can be extended for real-time disease surveillance. Data were obtained from an  
191 existing program implemented in 2018 to assess facility use and student engagement, in order  
192 to aid the university in allocation of resources. All students were alerted via a campus-wide  
193 notice about the program, and could choose to opt out; an overwhelming majority (98%)  
194 participated.

195  
196 Through an examination of campus-wide connectivity patterns, we identified associations  
197 between student activity and CMU's COVID-19-related policies. We found elevated on-campus  
198 presence during weekdays (vs. weekends) and in residence halls (vs. other building types) in  
199 fall 2020 (Appendix Figures 5, 6A, 6C), reflecting university policies that discouraged on-  
200 campus gathering. When mitigation policies relaxed in Spring 2021, weekend presence  
201 increased relative to fall 2020 (Appendix Figure 6B and 6D). Additionally, after testing positive,  
202 individuals had 42% fewer contacts than during the preceding 10 days, indicating adherence to  
203 isolation policies (Appendix Figure 7A). This quantification of policy adherence suggests that wifi  
204 datasets can be used to assess policy implementation or to determine the effects of policy  
205 updates in real time.

206  
207 We found that positive individuals exhibited distinct patterns in their social networks and  
208 behaviors. Individuals who eventually tested positive exhibited larger social networks than those  
209 who remained negative: they spent more days on campus (Appendix Figure 7B), had more daily  
210 contacts (Figure 3A, left), and interacted for a longer duration with each contact (Figure 3A,  
211 right), creating more opportunities for potential viral transmission. Furthermore, in the 10 days  
212 preceding both of their positive tests, pairs of students identified *via* contact tracing had  
213 significantly longer daily interaction times than other pairs of positive students (*e.g.*, median of

214 104 vs. 45 minutes per interaction per day in the fall; Appendix Figure 7CD). Moreover, these  
215 pairs of positive students between whom COVID-19 transmission may have occurred interacted  
216 for significantly longer than for pairs in which transmission did not or could not have occurred  
217 (*i.e.*, pairs involving one or more students who never tested positive; Appendix Figure 7CD).  
218 These distinct qualities support supplementing, and if necessary substituting, manual contact  
219 tracing with a wifi-based system to automatically flag close contacts of positive individuals.

220  
221 We further explored interactions between positive and negative individuals using the attribute  
222 assortativity metric (AA), which quantifies the extent to which individuals interact within-group  
223 vs. between-group compared to random assortment (Figure 3B). We found that both positive  
224 (*i.e.*, individuals positive at any point over the semester) and pre-positive individuals (*i.e.*,  
225 individuals within 10 days of a positive test) were more likely to associate with one another than  
226 with negative individuals (Figure 3C, Appendix Figure 8A–C). Importantly, this relationship  
227 remained significant, albeit with a lower effect size, when removing pre-positive individuals who  
228 identified one another as close contacts, suggesting that this finding is not limited to positive  
229 individuals identified via reflexive testing secondary to manual contact tracing (Appendix Figure  
230 9). Interestingly, the AA for pre-positive individuals was a leading indicator of daily case counts,  
231 by 8 days (Fall) and 3 days (Spring; Figure 3DE, Appendix Figure 8D–F), suggesting that the  
232 degree of within-group interactions among putatively infectious individuals increases in the days  
233 leading to these individuals' positive tests.

#### 234 4. Phylogenetic analysis of clinical viral genomes identified cluster size 235 overdispersion and cryptic transmissions, leading to concrete policy decisions

236 Viral genomic sequencing from residual biomaterial enables exploration of transmission  
237 dynamics and rapid detection and monitoring of SARS-CoV-2 variants. At CMU, sequencing  
238 facilitated detection of 18 distinct Pango lineages (Figure 4A; Appendix Figure 2BC)<sup>34</sup>. Of these,  
239 B.1.2 was the most abundant both at CMU and in Colorado, reflecting circulation between CMU  
240 and the surrounding community and highlighting the importance of CMU's sponsored testing for  
241 Mesa County<sup>35</sup>. We identified continuous transmission of this lineage between semesters, with 7  
242 spring cases descending from 17 fall cases as the likely result of 2–3 cryptic intermediate  
243 transmissions during winter recess<sup>36</sup>. This cluster was non-significantly enriched for off-campus  
244 students relative to the remaining sequenced cases (83% vs. 70% off-campus;  $p = 0.15$ );  
245 possible off-campus continuation of the transmission chain over the break suggests that  
246 institutional surveillance programs would be wise to maintain testing availability for nearby  
247 students during school breaks.

248  
249 We detected overdispersion in both genomic and social clustering data, highlighting the  
250 importance of policies that minimize super-spreading events. Of 41 detected introductions to the  
251 university, onward transmission was only observed from 13, with 5 of the resulting clusters  
252 containing 80% of sequenced cases ( $k=0.12$  in a negative binomial model, consistent with other  
253 studies<sup>37,38</sup>; Figure 4BC). We also observed overdispersion in the number of contacts between  
254 individuals in both contact tracing and wifi proximity analyses, where 80% of reported contacts  
255 were made by 33% ( $k=0.83$ ) and 43% ( $k=0.89$ ) of positive individuals, respectively (Figure  
256 4DE). The similar shape of these contact distributions suggests that both datasets capture the

257 true underlying structure of social interactions. Notably, phylogenomic cluster size demonstrates  
258 greater overdispersion than the two contact count distributions, suggesting that overdispersion  
259 in SARS-CoV-2 transmission can be partitioned into both social and biological components.  
260 Given the high variance observed amongst all three distributions, we suggest that both  
261 biological and social factors influence large SARS-CoV-2 case clusters, and that their interplay  
262 warrants further investigation. Below, we investigate the impact of a variety of variables on a  
263 distinct spring cluster.

## 264 5. Contemporaneous wastewater viral sequencing supplements lineage detection 265 and enables detection of emergent mutations

266 During 6 weeks from February to mid-March 2021, we obtained 42 wastewater samples from 10  
267 sites for sequencing, 9 of which were sequenced in duplicate (Appendix Figure 3C). The  
268 concurrent collection of wastewater samples and clinical specimens, with high breadth of  
269 coverage among the residential population, allowed us to directly compare viral sequences from  
270 wastewater with those from contemporaneous individual cases. Through this, we validated the  
271 utility of wastewater viral sequencing as a component of a comprehensive pathogen  
272 surveillance program, as currently instantiated by *Lookout*.

273  
274 As expected, wastewater viral titers were lower than titers of clinical specimens collected from  
275 upstream individuals (Appendix Figure 10A). Wastewater and clinical samples from CMU had  
276 similar sequence coverage, suggesting that there was no particular bias in viral RNA  
277 degradation in wastewater (Appendix Figure 10B–E). This demonstrates that these wastewater  
278 samples were comparable to clinical specimens in integrity and suitable for sequencing and  
279 genomic surveillance.

280  
281 We used the pre-existing Freyja tool<sup>39,40</sup> to detect 8 lineages in wastewater, 3 of which were  
282 found in concurrent clinical cases (Figure 5C, Appendix Table 6). Another 3 were observed in  
283 clinical cases prior to wastewater collection, suggesting undetected circulation on campus,  
284 shedding from previously-infected individuals, or environmental persistence. The remaining 2,  
285 B.1.533 and B.1.350, were present in the US but not the campus or state<sup>35</sup>; each was detected  
286 at low abundance in single samples and likely originated from a small number of individuals.  
287 Wastewater sequencing thus identified lineages not concurrently detected via clinical  
288 sequencing, proving itself to be particularly relevant in instances of incomplete clinical genomic  
289 sampling.

290  
291 In addition to detection of defined lineages, wastewater sequencing can also identify novel  
292 mutations; for this latter use case, we found that quality control mechanisms were essential to  
293 identify true variation. Of 1521 wastewater single nucleotide variants (SNVs), 85% and 68%  
294 were not found at consensus-level in CMU and Colorado clinical samples, respectively, and only  
295 4% were derived from clinical minor alleles (Figure 5D). We thus hypothesized that many  
296 mutations arose from amplification errors (e.g., formation of chimeras), a theory supported by  
297 the order-of-magnitude difference in the number of SNVs detected in wastewater vs. clinical  
298 samples as a function of sample count (Appendix Figure 11). We subsequently developed  
299 quality control methods to corroborate mutations *via* detection in state-wide clinical genomes.

300 We achieved high specificity for discarding SNVs not seen in Colorado when we required  
301 presence in both of two technical replicates (specificity = 98%) or an allele frequency exceeding  
302 25% (specificity = 92%); both methods had low sensitivity (50% and 62%, respectively; Figure  
303 5E), as each excluded SNVs corroborated by clinical viral genomes. This analysis provides real-  
304 word evidence of the importance of replicates for identifying true SNVs in wastewater samples,  
305 a finding previously shown for clinical minor allele validation<sup>41</sup>.

306  
307 Of 68 replicate-corroborated SNVs found across 9 wastewater samples with 2 technical  
308 replicates, 11 (16%) were not seen in clinical CMU samples (Appendix Table 7). 6 of the 11  
309 were present in Colorado and had allele frequencies >96% in single wastewater specimens,  
310 likely reflecting on-campus circulation of viral genotypes unsampled by clinical sequencing. Of  
311 the 5 remaining mutations, 2 were non-synonymous mutations in ORF1ab (I1970S, T3462I) and  
312 were novel compared with published global variation<sup>35</sup>, 2 were synonymous mutations, and 1  
313 was a premature stop codon. The latter mutation, with an allele frequency of 4%, may be  
314 spurious; the other 4, with allele frequencies between 27% and 100%, could reflect either gut  
315 tropism or cryptic transmission. Though these mutations' phenotypic effects remain unknown,  
316 their identification serves as a proof-of-concept and provides a framework for detection of novel  
317 mutations in wastewater.

## 318 6. Detection of novel lineage B.1.429.1 on campus leads to high-resolution 319 characterization of social and biological factors implicated in its spread

320 In Spring 2021, we detected a cluster of cases on campus that was concerning due to its  
321 unprecedented size and genomic ancestry, and proceeded to characterize it analytically and  
322 experimentally to identify the social and biological factors that contributed to its rise. This  
323 B.1.429.1 cluster initiated as a single introduction to campus, which proliferated into several  
324 star-like descendant sub-clusters, consistent with clonal amplification (Figure 6A). In total, the  
325 outbreak lasted for 45 days; in its final 4 weeks, it represented 33% of sequenced clinical  
326 samples and was the most abundant lineage in 47% of wastewater samples (Figure 6AB).  
327 B.1.429.1 descended from B.1.429 – then deemed a Variant of Concern due to reduced  
328 antibody neutralization and increased viral shedding, infectivity, and transmissibility<sup>42</sup> – but also  
329 included the recurrent S:Q677H substitution, posited to further increase transmissibility<sup>43</sup>  
330 (Appendix Table 8).

331  
332 We did not detect differences in interaction patterns among individuals with B.1.429.1 vs. those  
333 with other viral lineages (Appendix Figure 12AB), suggesting that its transmissibility was due to  
334 inherent qualities of the lineage rather than the specific social dynamics of the individuals within  
335 the cluster. We did find that these individuals clustered together in social networks (Figure 6C);  
336 *i.e.*, they were on average one social connection closer to one another than to other positive  
337 individuals ( $p < 0.001$ ). Wifi-connected B.1.429.1 pairs also had significantly lower genetic  
338 distances between their viral genomes than non-connected B.1.429.1 pairs (Figure 6D),  
339 demonstrating that connections observed within the wifi network are enriched for genuine  
340 transmission events.

341



342 We inferred direct transmission links among B.1.429.1 cases and found that wifi connectivity  
343 data inferred transmission networks that paralleled those constructed following traditional  
344 contact tracing. Alone, manual contact tracing or genomic sequencing resolved transmission  
345 links for 61% and 68% of individuals, respectively (Appendix Figure 12DE). We thus combined  
346 genomic data with traditional contact (2 days prior to tests) or wifi-derived contract tracing (for  
347 both 2 and 10 days prior to tests), producing transmission models connecting 82%, 87%, and  
348 74% of sequenced cases, respectively (Figure 6EF, Appendix Figure 12F). We compared the  
349 cluster topology for these networks and found that the wifi 10-day data best approximated the  
350 traditional contact tracing network (*via* Jaccard distance; Appendix Table 10). Due to the paucity  
351 of distinguishing mutations present between individual consensus mutations<sup>44</sup>, we used  
352 intrahost viral variation to supplement our transmission linkages. We identified a clear  
353 transmission chain where a single mutation present at low frequency in one specimen (#26 in  
354 Figure 6EF) reached fixation in two specimens (#27 & 28 in Figure 6EF) collected one week  
355 later, consistent with bottlenecked transmission. These three individuals clustered together in all  
356 reconstruction networks, but without the directionality of transmission inferred from minor alleles  
357 or phylogenetic descent, implying that transmission network reconstruction tools would benefit  
358 from further refinement.

359  
360 We next analyzed inherent phenotypic factors that could explain the increased transmission of  
361 B.1.429.1 on campus. We assessed the impact of the S:Q677H mutation found in B.1.429.1 on  
362 single-cycle infectivity and on cell-to-cell fusogenicity in lentiviral pseudotypes (Appendix Figure  
363 12GH). While the mutation did not alter virion spike protein levels or cell-free virion infectivity  
364 (Appendix Figure 12C), it significantly increased fusion efficiency relative to the ancestral  
365 B.1.429 spike protein (Figure 6G), likely due to proximity to the spike protein polybasic cleavage  
366 site. We found similar results for the S:Q677P mutation, which was detected in other  
367 contemporaneous CMU lineages. This finding is consistent with greater within-host  
368 dissemination of SARS-CoV-2 haplotypes bearing S:Q677H or S:Q677P.

369  
370 Fortunately, B.1.429.1 was minimally detected outside the campus, pointing to the success of  
371 CMU's containment policies. This vignette highlights the power of systematic, multimodal  
372 surveillance programs to not only identify and mitigate transmission events, but also to  
373 contribute to novel biological characterization of viral lineages.

## 374 Discussion

375 In this paper, we analyzed clinical diagnostic data, case attributes, wifi co-location logs,  
376 wastewater samples, and viral genomic sequences to quantify the success of CMU's pandemic  
377 response program and to assess the relevance of each data type for infectious disease  
378 surveillance. Our analyses showed that through contact tracing, wastewater surveillance, and  
379 increased focus on high-risk groups, CMU effectively identified positive cases. Via novel  
380 analyses of wifi connectivity, we confirmed adherence to school policies and evaluated metrics  
381 that could allow wifi data to replace or supplement traditional contact tracing.

382  
383 In addition, we leveraged phylogenetic and epidemiological analyses to propose future policies  
384 to limit disease spread (*e.g.*, continued testing during school breaks, community testing, risk

385 prediction for testing prioritization) and to identify and mitigate specific causal factors shown to  
386 increase risk (e.g., requiring high-quality masking or increased testing to participate in high-  
387 contact sports). Our sequencing of extant wastewater samples not only identified lineages  
388 independently of clinical sequencing, but also led us to apply and verify methodological  
389 procedures necessary for the detection of novel mutations from wastewater. Finally, through  
390 analysis of case cluster overdispersion and the novel lineage B.1.429.1, we highlighted the  
391 relevance of investigating both virological and sociobehavioral factors that can influence  
392 transmission.

393  
394 Our results lead us to formulate a framework combining the analyzed tools within an integrated  
395 disease surveillance system (described in Figure 7). First, we emphasize beginning with  
396 mitigation policies such as symptom reporting, contact tracing, and quarantine and continuing  
397 with efficient testing strategies such as wastewater surveillance. While contact tracing is  
398 essential, it is also time-intensive and expensive to maintain; with further work to address  
399 technological and privacy concerns, wifi proximity and geolocation data could supplement and  
400 perhaps ultimately replace these efforts. Gathering epidemiological metadata, symptom  
401 attestations, and diagnostic test results digitally and with programmatic synthesis is also a high  
402 priority because it can facilitate real-time analyses and subsequent policy adjustments; the  
403 *Lookout* system serves as a useful template (Figure 1)<sup>30</sup>. If finances allow, we would add  
404 genomic surveillance to aid identification of transmission patterns and concerning lineages or  
405 mutations. For communities with wastewater surveillance, sequencing these samples provides a  
406 cheaper alternative to clinical sequencing of all upstream individuals and still allows for  
407 identification of lineages or mutations of interest. This tool cannot wholly replace clinical  
408 sequencing due to its inability to discern transmission trends. It is important to emphasize that  
409 disease surveillance is not a one-size-fits-all endeavor; in fact, we found parallel results across  
410 data types. We suggest that automated integration of a subset of data types will more powerfully  
411 combat infectious disease outbreaks than a siloed implementation of all data types.

412  
413 Our findings are subject to statistical, methodological, and policy-based limitations. As with all  
414 studies of infectious disease surveillance, transmission events and clustering can violate  
415 statistical assumptions of independence among individuals. Additionally, while CMU had access  
416 to attribute data for individuals who never tested positive in the *Lookout* system, we were unable  
417 to access it for research under our existing regulatory approval; this impeded our ability to  
418 separate the impact that individual attributes (e.g., a particular sports team or residence hall)  
419 had on risk of infection. Moreover, incomplete sampling of residual diagnostic biospecimen and  
420 wastewater samples limited us to a partial snapshot of SARS-CoV-2 genetic diversity at CMU  
421 (Figure 2A; Appendix Figure 3C). Further, wifi co-location logs remain an underexplored data  
422 source that does not capture off-campus interactions and likely records superfluous or false  
423 interactions. As our study largely took place prior to the widespread availability of SARS-CoV-2  
424 vaccines<sup>45</sup> and of rapid at-home antigen tests<sup>46</sup>, we cannot assess their impact on infectious  
425 disease transmission or policy. Finally, CMU's surveillance paradigm prioritized community  
426 safety over individual privacy; thus, some of our findings may not be generalizable to institutions  
427 with different prioritizations.

428

429 Accounting for resource constraints, we built upon CMU's community-driven mindset to develop  
430 an efficient surveillance program and lay the groundwork for future advances. While a number  
431 of analyses here were conducted only retrospectively, updates to surveillance software like  
432 *Lookout*<sup>30</sup> could enable timely identification of risk factors for infection and spread, proximity and  
433 location patterns, and lineages or mutations that are rising in frequency or that have been  
434 categorized as Variants of Concern. They could further refine the accuracy of outbreak  
435 reconstruction by incorporating genomic data including major and minor alleles, and contact  
436 tracing obtained from manual efforts or wifi analyses, with reported contacts weighted by the  
437 length or nature of the interaction. In summary, we propose the seamless, automated  
438 integration of multiple data types as the most powerful way to combat infectious disease  
439 outbreaks as they unfold.

## 440 Methods

441 Code associated with the analyses of this study is available at:  
442 <https://github.com/broadinstitute/sc2-cmu-study>. Detailed methods are included in an appendix.

443  
444 We identified factors associated with testing positive for SARS-CoV-2 *via* calculation of 1)  
445 relative risk for athletic participation, campus residency, and sex, and 2) Pearson's chi-square  
446 test for distinct sports teams, residence halls, and class years. We also fit a linear model to  
447 residence hall incidence rates as a function of various binary and continuous attributes of the  
448 buildings (Appendix Figure 4A).

449  
450 We examined differences in daily wifi connectivity patterns between subgroups defined by  
451 infection status or viral lineage and quantified differences in relevant metrics (Appendix Table  
452 11) across subgroups via the Mann-Whitney U test. We calculated attribute assortativity (AA) to  
453 assess the tendency of individuals to associate with in-group *vs.* across groups, and determined  
454 the lag time that maximizes the correlation between AA and case count.

455  
456 We constructed a network of known positive individuals, and connected pairs of individuals with  
457 interactions within 10 days of both positive tests. We compared wifi network path distances (i.e  
458 cumulative number of edges on the shortest path connecting two individuals in the network)  
459 between individuals in each pair where both were infected with B.1.429.1 lineage virus against  
460 pairs where only one individual had this viral lineage. We next compared viral genome distances  
461 (i.e., number of SNVs) within pairs of individuals infected with B.1.429.1 lineage virus that were  
462 connected by a path in the network *vs.* not connected.

463  
464 Rolling 24-hour wastewater aliquots were collected from sewer sites to (1) monitor SARS-CoV-2  
465 concentration via RT-qPCR and (2) provide source material for viral genomic sequencing.  
466 Across all collection sites, we compared weekly case counts from source buildings against daily  
467 and weekly wastewater viral titers (via Spearman correlation and Fisher's exact test,  
468 respectively).

469  
470 Excess material from clinical diagnostic tests and wastewater aliquots was sequenced following  
471 enrichment via PCR with ARTICv3-tiled amplicons.

472  
473 LoFreq was used to call major and minor alleles within wastewater samples. Several quality  
474 control metrics were considered to discard spurious variation: minimum allele frequency, local  
475 sequencing depth, and concordance in variation across replicates<sup>47</sup>. Freyja was used to identify  
476 and estimate the abundance of constituent SARS-CoV-2 lineages<sup>39</sup>. We determined the  
477 average number of unique SNVs that a single additional sequenced sample contributes to a set  
478 of a given number of samples, via bootstrapping of distinct subsets of clinical or wastewater  
479 samples.

480  
481 Clinical genomes were assembled using the Broad Institute viral-ngs pipelines and Nextstrain  
482 pipelines and assigned Pango lineages<sup>34,48</sup>. Genomes were placed in the phylogenetic context  
483 of genomes from cases outside the university community, weighted toward genomes from  
484 Colorado and surrounding states. Case clusters were identified based on a state change from  
485 not university-associated to university-associated, following ancestral state reconstruction of  
486 internal tree nodes.

487  
488 Negative binomial distributions were fit to distributions of cluster size, the number of contacts in  
489 the wifi data set, and the number of contacts in the standard contact tracing data set. Contacts  
490 were defined as any interaction >15 minutes in the 48-hour period prior to testing or symptom  
491 onset.

492  
493 Transmission networks were inferred using sequenced viral genomes and contact data using  
494 *outbreaker2*<sup>49</sup>.

495  
496 Lentiviral pseudotype assays were performed to assess the functional implications of the  
497 S:Q677H substitution on infectivity and fusogenicity.

## 498 Funding Acknowledgments

499 This work was supported by the National Science Foundation (NSF) Graduate Research  
500 Fellowship Program to J.S.P. (grant number 1745303), and C.H.T-T. (grant number 1745303);  
501 the Hertz Foundation to J.S.P.; the National Institute of General Medical Sciences to B.A.P.  
502 (grant number T32GM007753); the National Science Foundation (NSF) to B.C.L. (grant number  
503 2046440); the Moore Foundation to B.C.L., the National Institute of Allergy and Infectious  
504 Diseases to B.C.L. (grant number 2U19AI110818) and to P.C.S. (grant number U19AI110818  
505 and U01AI151812); the National Institutes of Health to J.L. (grant numbers R37AI147868 and  
506 R01AI148784); the Massachusetts Consortium on Pathogen Readiness to J.L.; the Centers for  
507 Disease Control and Prevention (CDC) COVID-19 baseline genomic surveillance contract to the  
508 Clinical Research Sequencing Platform (grant number 75D30121C10501) and a CDC Broad  
509 Agency Announcement to B.L.M. (grant number 75D30120C09605); and the Howard Hughes  
510 Medical Institute to P.C.S. This work is also made possible by support from Flu Lab and a  
511 cohort of donors through the Audacious Project, a collaborative funding initiative housed at  
512 TED, including The ELMA Foundation, MacKenzie Scott, the Skoll Foundation, and Open  
513 Philanthropy.

514 Any opinion, findings, and conclusions or recommendations expressed in this material are those  
515 of the author(s) and do not necessarily reflect the views of the National Science Foundation.

516 This content is solely the responsibility of the authors and does not necessarily represent the  
517 official views of the National Institute of General Medical Sciences or the National Institutes of  
518 Health.

## 519 Acknowledgements

520 The authors wish to thank Jacob E. Lemieux for helpful discussions and feedback. The authors  
521 also wish to thank Laurent Hébert-Dufresne for providing insights and feedback on the wifi co-  
522 location analyses.

## 523 Conflicts of Interest

524 P.C.S. is a co-founder of, shareholder in, and scientific advisor to Sherlock Biosciences, Inc;  
525 she is also a Board member of and shareholder in Danaher Corporation. P.C.S. has filed IP  
526 related to genome sequencing and analysis.

## 527 Ethics Statement

528 The study was conducted at the Broad Institute with approval from the MIT Institutional Review  
529 Board under Protocol #1612793224 and from WCG IRB Protocol #20210166 under Protocol:  
530 Investigating Viral Emergence and Spread in Community Settings.

## 531 References

- 532 1. Shah, M., Quinlisk, P., Weigel, A., Riley, J., James, L., Patterson, J., Hickman, C., Rota,  
533 P.A., Stewart, R., Clemmons, N., et al. (2018). Mumps Outbreak in a Highly Vaccinated  
534 University-Affiliated Setting Before and After a Measles-Mumps-Rubella Vaccination  
535 Campaign-Iowa, July 2015-May 2016. *Clin. Infect. Dis.* 66, 81–88.
- 536 2. Harrison, L.H., Dwyer, D.M., Maples, C.T., and Billmann, L. (1999). Risk of meningococcal  
537 infection in college students. *JAMA* 281, 1906–1910.
- 538 3. Delbos, V., Lemée, L., Bénichou, J., Berthelot, G., Taha, M.-K., Caron, F., and B14 STOP  
539 study group (2013). Meningococcal carriage during a clonal meningococcal B outbreak in  
540 France. *Eur. J. Clin. Microbiol. Infect. Dis.* 32, 1451–1459.
- 541 4. MacLennan, J., Kafatos, G., Neal, K., Andrews, N., Cameron, J.C., Roberts, R., Evans,  
542 M.R., Cann, K., Baxter, D.N., Maiden, M.C.J., et al. (2006). Social behavior and  
543 meningococcal carriage in British teenagers. *Emerg. Infect. Dis.* 12, 950–957.
- 544 5. Segaloff, H.E., Cole, D., Rosenblum, H.G., Lee, C.C., Morgan, C.N., Remington, P., Pitts,  
545 C., Kelly, P., Baggott, J., Bateman, A., et al. (2021). Risk Factors for Severe Acute  
546 Respiratory Syndrome Coronavirus 2 (SARS-CoV-2) Infection and Presence of Anti-SARS-  
547 CoV-2 Antibodies Among University Student Dormitory Residents, September-November  
548 2020. *Open Forum Infect Dis* 8, ofab405.
- 549 6. Vang, K.E., Krow-Lucal, E.R., James, A.E., Cima, M.J., Kothari, A., Zohoori, N., Porter, A.,  
550 and Campbell, E.M. (2021). Participation in Fraternity and Sorority Activities and the  
551 Spread of COVID-19 Among Residential University Communities - Arkansas, August 21-

- 552 September 5, 2020. *MMWR Morb. Mortal. Wkly. Rep.* 70, 20–23.
- 553 7. Nolan, T., O’Ryan, M., Wassil, J., Abitbol, V., and Dull, P. (2015). Vaccination with a  
554 multicomponent meningococcal B vaccine in prevention of disease in adolescents and  
555 young adults. *Vaccine* 33, 4437–4445.
- 556 8. Prater, K.J., Fortuna, C.A., McGill, J.L., Brandeberry, M.S., Stone, A.R., and Lu, X. (2016).  
557 Poor hand hygiene by college students linked to more occurrences of infectious diseases,  
558 medical visits, and absence from classes. *Am. J. Infect. Control* 44, 66–70.
- 559 9. Lu, H., Weintz, C., Pace, J., Indana, D., Linka, K., and Kuhl, E. (2021). Are college  
560 campuses superspreaders? A data-driven modeling study. *Comput. Methods Biomech.*  
561 *Biomed. Engin.* 24, 1136–1145.
- 562 10. Valesano, A.L., Fitzsimmons, W.J., Blair, C.N., Woods, R.J., Gilbert, J., Rudnik, D.,  
563 Mortenson, L., Friedrich, T.C., O’Connor, D.H., MacCannell, D.R., et al. (2021). SARS-  
564 CoV-2 Genomic Surveillance Reveals Little Spread From a Large University Campus to the  
565 Surrounding Community. *Open Forum Infect Dis* 8, ofab518.
- 566 11. Crowe, J., Schnaubelt, A.T., Schmidt-Bonne, S., Angell, K., Bai, J., Eske, T., Nicklin, M.,  
567 Pratt, C., White, B., Crotts-Hannibal, B., et al. (2021). Pilot program for test-based SARS-  
568 CoV-2 screening and environmental monitoring in an urban public school district. *bioRxiv*.
- 569 12. Petros, B.A., Turcinovic, J., Welch, N.L., White, L.F., Kolaczyk, E.D., Bauer, M.R., Cleary,  
570 M., Dobbins, S.T., Doucette-Stamm, L., Gore, M., et al. (2022). Early introduction and rise  
571 of the Omicron SARS-CoV-2 variant in highly vaccinated university populations. *Clin. Infect.*  
572 *Dis.*
- 573 13. Rennert, L., and McMahan, C. (2021). Risk of Severe Acute Respiratory Syndrome  
574 Coronavirus 2 (SARS-CoV-2) Reinfection in a University Student Population. *Clin. Infect.*  
575 *Dis.*
- 576 14. Paltiel, A.D., Zheng, A., and Walensky, R.P. (2020). Assessment of SARS-CoV-2  
577 Screening Strategies to Permit the Safe Reopening of College Campuses in the United  
578 States. *JAMA Netw Open* 3, e2016818.
- 579 15. Stubbs, C.W., Springer, M., and Thomas, T.S. (2020). The impacts of testing cadence,  
580 mode of instruction, and student density on fall 2020 covid-19 rates on campus. *medRxiv*.
- 581 16. Frazier, P.I., Cashore, J.M., Duan, N., Henderson, S.G., Janmohamed, A., Liu, B., Shmoys,  
582 D.B., Wan, J., and Zhang, Y. (2022). Modeling for COVID-19 college reopening decisions:  
583 Cornell, a case study. *Proc. Natl. Acad. Sci. U. S. A.* 119.
- 584 17. Queen, C.S., and Allen, J. (2021). 100 U.S. colleges will require vaccinations to attend in-  
585 person classes in the fall. *The New York Times*.
- 586 18. Karthikeyan, S., Nguyen, A., McDonald, D., Zong, Y., Ronquillo, N., Ren, J., Zou, J.,  
587 Farmer, S., Humphrey, G., Henderson, D., et al. (2021). Rapid, Large-Scale Wastewater  
588 Surveillance and Automated Reporting System Enable Early Detection of Nearly 85% of  
589 COVID-19 Cases on a University Campus. *mSystems* 6, e0079321.
- 590 19. Shah, M., Ferra, G., Fitzgerald, S., Barreira, P.J., Sabeti, P.C., and Colubri, A. (2022).

- 591           Containing the spread of mumps on college campuses. *R Soc Open Sci* 9, 210948.
- 592   20. Sabeti, P., Botti-Lodovico, Y., Baruch, J., Gutiérrez-Ramos, J.-C., Aguilar, M., Wosen, J.,  
593   Feuerstein, A., Garde, D., and Herper, M. (2020). A mumps epidemic has a lot to teach  
594   colleges about reopening safely in the time of coronavirus. *STAT*.  
595   [https://www.statnews.com/2020/10/08/a-mumps-epidemic-has-a-lot-to-teach-colleges-](https://www.statnews.com/2020/10/08/a-mumps-epidemic-has-a-lot-to-teach-colleges-about-reopening-safely-in-the-time-of-coronavirus/)  
596   [about-reopening-safely-in-the-time-of-coronavirus/](https://www.statnews.com/2020/10/08/a-mumps-epidemic-has-a-lot-to-teach-colleges-about-reopening-safely-in-the-time-of-coronavirus/).
- 597   21. Currie, D.W., Moreno, G.K., Delahoy, M.J., Pray, I.W., Jovaag, A., Braun, K.M., Cole, D.,  
598   Shechter, T., Fajardo, G.C., Griggs, C., et al. (2021). Interventions to Disrupt Coronavirus  
599   Disease Transmission at a University, Wisconsin, USA, August-October 2020. *Emerg.*  
600   *Infect. Dis.* 27, 2776–2785.
- 601   22. Matrajt, L., and Leung, T. (2020). Evaluating the Effectiveness of Social Distancing  
602   Interventions to Delay or Flatten the Epidemic Curve of Coronavirus Disease. *Emerg.*  
603   *Infect. Dis.* 26, 1740–1748.
- 604   23. Kim, M.-C., Kweon, O.J., Lim, Y.K., Choi, S.-H., Chung, J.-W., and Lee, M.-K. (2021).  
605   Impact of social distancing on the spread of common respiratory viruses during the  
606   coronavirus disease outbreak. *PLoS One* 16, e0252963.
- 607   24. Glass, R.J., Glass, L.M., Beyeler, W.E., and Min, H.J. (2006). Targeted Social Distancing  
608   Designs for Pandemic Influenza. *Emerging Infectious Disease journal* 12, 1671.
- 609   25. Tang, S., Xiao, Y., Yuan, L., Cheke, R.A., and Wu, J. (2012). Campus quarantine  
610   (Fengxiao) for curbing emergent infectious diseases: lessons from mitigating A/H1N1 in  
611   Xi'an, China. *J. Theor. Biol.* 295, 47–58.
- 612   26. Harris-Lovett, S., Nelson, K.L., Beamer, P., Bischel, H.N., Bivins, A., Bruder, A., Butler, C.,  
613   Camenisch, T.D., De Long, S.K., Karthikeyan, S., et al. (2021). Wastewater Surveillance for  
614   SARS-CoV-2 on College Campuses: Initial Efforts, Lessons Learned, and Research Needs.  
615   *Int. J. Environ. Res. Public Health* 18.
- 616   27. Fielding-Miller, R., Karthikeyan, S., Gaines, T., Garfein, R.S., Salido, R., Cantu, V., Kohn,  
617   L., Martin, N.K., Wijaya, C., Flores, M., et al. (2021). Wastewater and surface monitoring to  
618   detect COVID-19 in elementary school settings: The Safer at School Early Alert project.  
619   medRxiv.
- 620   28. Das Swain, V., Xie, J., Madan, M., Sargolzaei, S., Cai, J., De Choudhury, M., Abowd, G.D.,  
621   Steimle, L.N., and Prakash, B.A. (2021). Empirical networks for localized COVID-19  
622   interventions using WiFi infrastructure at university campuses. bioRxiv.
- 623   29. Malloy, M.L., Hartung, L., Wangen, S., and Banerjee, S. (2022). Network-Side Digital  
624   Contact Tracing on a Large University Campus. arXiv [cs.NI].
- 625   30. Anthes, E. (2021). The Future of Virus Tracking Can Be Found on This College Campus.  
626   The New York Times.
- 627   31. Specht, I., Sani, K., Botti-Lodovico, Y., Hughes, M., Heumann, K., Bronson, A., Marshall, J.,  
628   Baron, E., Parrie, E., Glennon, O., et al. (2022). The case for altruism in institutional  
629   diagnostic testing. *Sci. Rep.* 12, 1857.

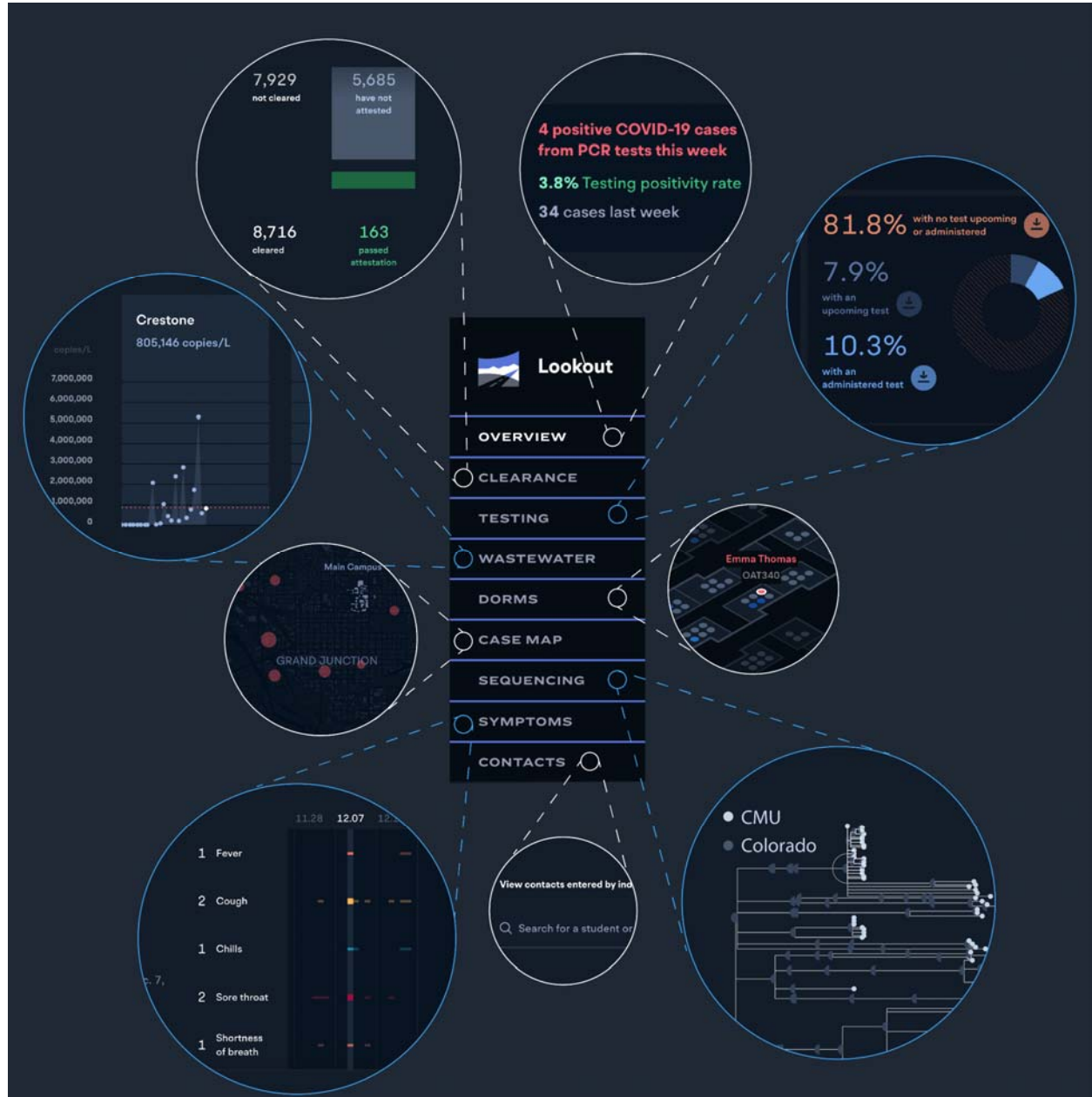
- 630 32. Student profiles [https://www.coloradomesa.edu/institutional-research/student-](https://www.coloradomesa.edu/institutional-research/student-profiles/index.html)  
631 profiles/index.html.
- 632 33. Lei, H., Xu, X., Xiao, S., Wu, X., and Shu, Y. (2020). Household transmission of COVID-19-  
633 a systematic review and meta-analysis. *J. Infect.* 81, 979–997.
- 634 34. O’Toole, Á., Scher, E., Underwood, A., Jackson, B., Hill, V., McCrone, J.T., Colquhoun, R.,  
635 Ruis, C., Abu-Dahab, K., Taylor, B., et al. (2021). Assignment of epidemiological lineages in  
636 an emerging pandemic using the pangolin tool. *Virus Evol* 7, veab064.
- 637 35. Outbreak.Info outbreak.info. [https://outbreak.info/situation-](https://outbreak.info/situation-reports?pango=B.1.429&loc=USA_US-NV&loc=USA_US-CA&selected=USA_US-NV)  
638 reports?pango=B.1.429&loc=USA\_US-NV&loc=USA\_US-CA&selected=USA\_US-NV.
- 639 36. Zhang, J., Litvinova, M., Wang, W., Wang, Y., Deng, X., Chen, X., Li, M., Zheng, W., Yi, L.,  
640 Chen, X., et al. (2020). Evolving epidemiology and transmission dynamics of coronavirus  
641 disease 2019 outside Hubei province, China: a descriptive and modelling study. *Lancet*  
642 *Infect. Dis.* 20, 793–802.
- 643 37. Meyerowitz, E.A., Richterman, A., Gandhi, R.T., and Sax, P.E. (2021). Transmission of  
644 SARS-CoV-2: A Review of Viral, Host, and Environmental Factors. *Ann. Intern. Med.* 174,  
645 69–79.
- 646 38. Bi, Q., Wu, Y., Mei, S., Ye, C., Zou, X., Zhang, Z., Liu, X., Wei, L., Truelove, S.A., Zhang,  
647 T., et al. (2020). Epidemiology and transmission of COVID-19 in 391 cases and 1286 of  
648 their close contacts in Shenzhen, China: a retrospective cohort study. *Lancet Infect. Dis.*  
649 20, 911–919.
- 650 39. Freyja: Depth-weighted De-Mixing (Github).
- 651 40. Karthikeyan, S., Levy, J.I., De Hoff, P., Humphrey, G., Birmingham, A., Jepsen, K., Farmer,  
652 S., Tubb, H.M., Valles, T., Tribelhorn, C.E., et al. (2021). Wastewater sequencing uncovers  
653 early, cryptic SARS-CoV-2 variant transmission. medRxiv, 2021.12.21.21268143.
- 654 41. Grubaugh, N.D., Gangavarapu, K., Quick, J., Matteson, N.L., De Jesus, J.G., Main, B.J.,  
655 Tan, A.L., Paul, L.M., Brackney, D.E., Grewal, S., et al. (2019). An amplicon-based  
656 sequencing framework for accurately measuring intrahost virus diversity using PrimalSeq  
657 and iVar. *Genome Biol.* 20, 8.
- 658 42. Deng, X., Garcia-Knight, M.A., Khalid, M.M., Servellita, V., Wang, C., Morris, M.K.,  
659 Sotomayor-González, A., Glasner, D.R., Reyes, K.R., Gliwa, A.S., et al. (2021).  
660 Transmission, infectivity, and neutralization of a spike L452R SARS-CoV-2 variant. *Cell*  
661 184, 3426–3437.e8.
- 662 43. Hodcroft, E.B., Domman, D.B., Snyder, D.J., Oguntuyo, K.Y., Van Diest, M., Densmore,  
663 K.H., Schwalm, K.C., Femling, J., Carroll, J.L., Scott, R.S., et al. (2021). Emergence in late  
664 2020 of multiple lineages of SARS-CoV-2 Spike protein variants affecting amino acid  
665 position 677. medRxiv.
- 666 44. Wohl, S., Giles, J.R., and Lessler, J. (2021). Sample size calculation for phylogenetic case  
667 linkage. *PLoS Comput. Biol.* 17, e1009182.
- 668 45. Office of the Commissioner FDA takes key action in fight against COVID-19 by issuing



- 669 emergency use authorization for first COVID-19 vaccine. U.S. Food and Drug  
670 Administration. [https://www.fda.gov/news-events/press-announcements/fda-takes-key-](https://www.fda.gov/news-events/press-announcements/fda-takes-key-action-fight-against-covid-19-issuing-emergency-use-authorization-first-covid-19)  
671 [action-fight-against-covid-19-issuing-emergency-use-authorization-first-covid-19](https://www.fda.gov/news-events/press-announcements/fda-takes-key-action-fight-against-covid-19-issuing-emergency-use-authorization-first-covid-19).
- 672 46. Center for Devices, and Radiological Health At-Home OTC COVID-19 Diagnostic Tests.  
673 U.S. Food and Drug Administration. [https://www.fda.gov/medical-devices/coronavirus-](https://www.fda.gov/medical-devices/coronavirus-covid-19-and-medical-devices/home-otc-covid-19-diagnostic-tests)  
674 [covid-19-and-medical-devices/home-otc-covid-19-diagnostic-tests](https://www.fda.gov/medical-devices/coronavirus-covid-19-and-medical-devices/home-otc-covid-19-diagnostic-tests).
- 675 47. Wilm, A., Aw, P.P.K., Bertrand, D., Yeo, G.H.T., Ong, S.H., Wong, C.H., Khor, C.C., Petric,  
676 R., Hibberd, M.L., and Nagarajan, N. (2012). LoFreq: a sequence-quality aware, ultra-  
677 sensitive variant caller for uncovering cell-population heterogeneity from high-throughput  
678 sequencing datasets. *Nucleic Acids Res.* *40*, 11189–11201.
- 679 48. viral-pipelines (Github).
- 680 49. Campbell, F., Cori, A., Ferguson, N., and Jombart, T. (2019). Bayesian inference of  
681 transmission chains using timing of symptoms, pathogen genomes and contact data. *PLoS*  
682 *Comput. Biol.* *15*, e1006930.
- 683
- 684

1 **Figure 1**

2 Figure 1. The *Lookout* system implements real-time monitoring of COVID-19 cases, including  
3 spatial, longitudinal, and social patterns of disease burden

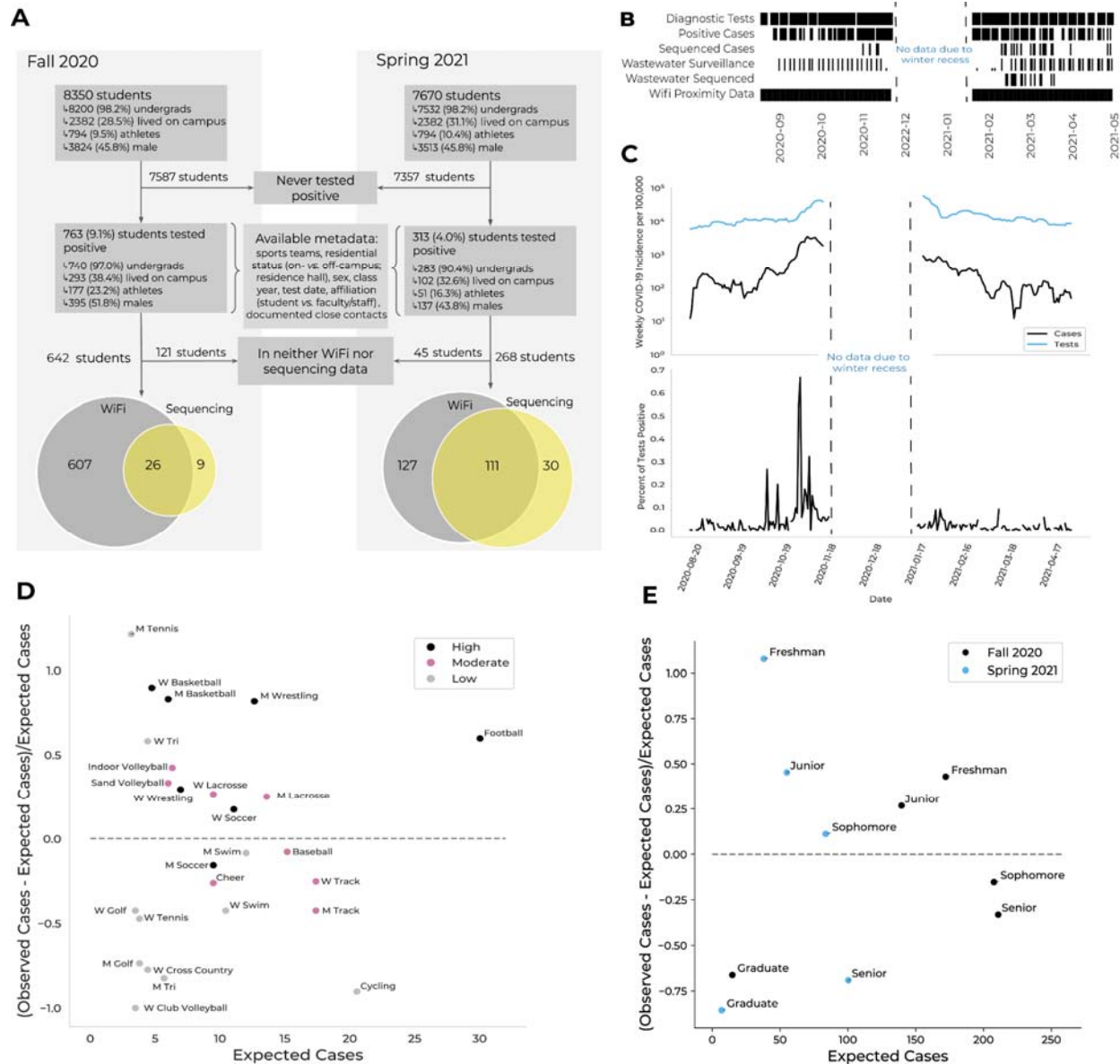


4 The *Lookout* tool integrated clinical diagnostic test results, student metadata, viral genome  
5 sequences from diagnostic specimens, and wastewater viral titers. A demo with representative  
6 synthetic data is available at <https://sentinel.network/lookout-demo-campus/>. **Overview.** Current  
7 data on community case burden, test volume, high-incidence groups, and symptom and  
8 exposure attestation. **Clearance.** Full-population counts of the individuals complying with the  
9 training and symptom attestation requirements for campus entry. **Testing.** Reports of positive  
10 tests in the past 7 days as well as the volume of tests scheduled, taken, and missed for the  
11

12 current week. **Testing - Baseline.** A view of “back to campus” testing measures tracking the  
13 number of tests administered over time against the amount needed to successfully test the  
14 entire population before a return to campus. **Wastewater.** Viral load over time, measured on a  
15 per-sewershed basis, aligned with individual test results from the same residence halls. **Dorms.**  
16 Views showing spatial position of residence hall cases on a per-floor basis. Individuals may be  
17 selected to view their associated membership groups (*i.e.*, potential close contacts), present  
18 attestation, test, and isolation status. Main view page depicts campus-wide case density. **Case**  
19 **Map.** Large-area view of case locations for members of the university community who live off-  
20 campus, with hot spots for locations of high case density. **Sequencing.** Phylogenetic tree  
21 showing the ancestry and clustering of viral genomes collected from university cases. Individual  
22 cases may be selected to view other individuals who are members of the same cluster, as well  
23 as specific attributes of the individual. Viral lineages are noted. **Symptoms.** Timelines depict  
24 reported symptoms for students or staff, including fever, cough, chills, sore throat, shortness of  
25 breath, loss of smell/taste, and runny nose. **Contacts.** Rapid search for the list of contacts  
26 reported by cases, and their associated contact information. **Lookup.** Review of information in  
27 *Lookout* for a given individual, including group affiliations, test result history, symptom history,  
28 attestation history, and contact history.

## 29 **Figure 2**

30 Figure 2. Data types, incidence rates, and epidemiological risk factors for SARS-CoV-2 positivity  
31 on Colorado Mesa University’s campus

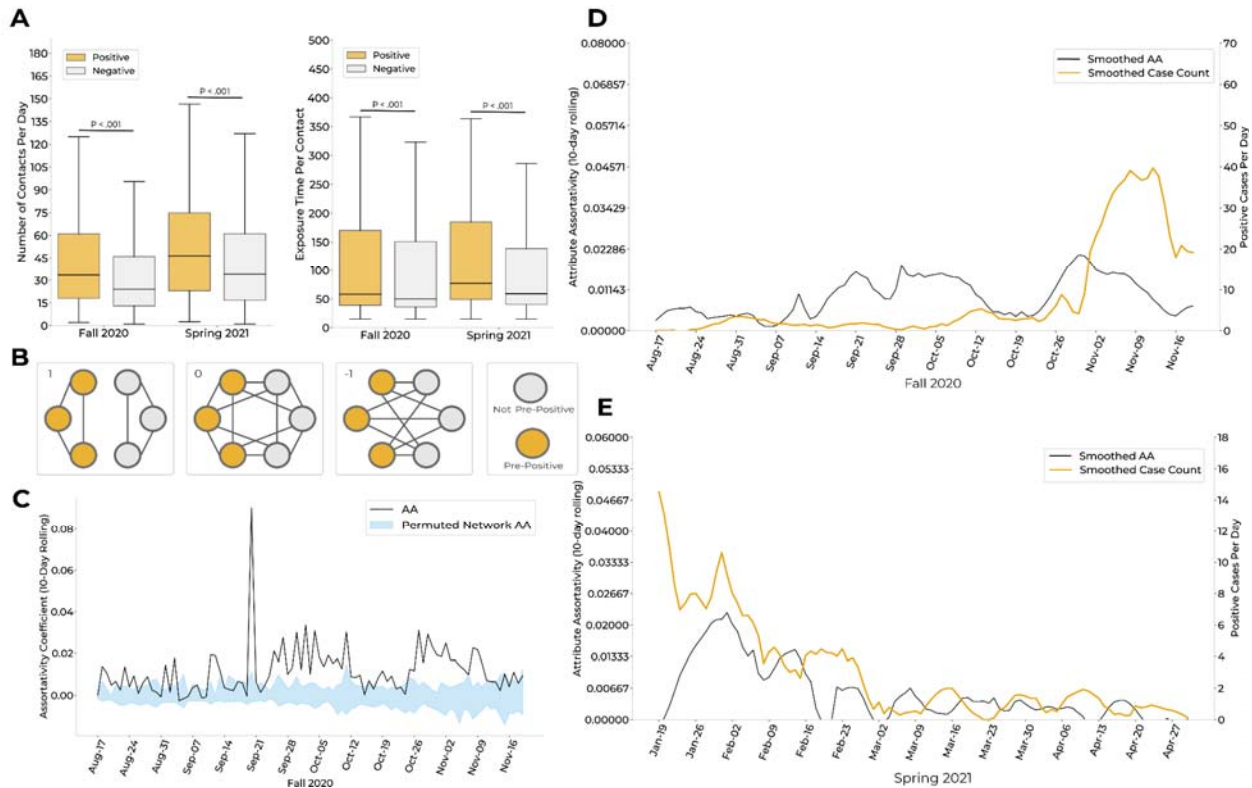


32  
 33 **A.** Cohort description. A subset of students at Colorado Mesa University (CMU) tested positive  
 34 for COVID-19 *via* reflexive or random surveillance RT-qPCR testing. CMU provided  
 35 demographic and behavioral metadata for each case. The majority of students who tested  
 36 positive were enrolled in the wifi proximity program (gray). A subset of positive samples were  
 37 available for viral genomic sequencing (yellow). **B.** Timeline showing data collection timepoints  
 38 (black) by data type during the Fall and Spring semesters. Data not shown for November 21–  
 39 January 18 due to winter recess. **C.** Upper: Weekly COVID-19 incidence (black) and number of  
 40 tests conducted (blue) over the 2020–2021 academic year. Lower: Percent positivity rate. Data  
 41 not shown for November 21–January 18 due to winter recess. **D.** The difference between the  
 42 number of cases observed and the number of cases expected (based on sports team player  
 43 count and scaled by the number of cases expected; y axis) vs. the number of cases expected (x  
 44 axis), per sports team. The dashed line at  $y=0$  separates teams with more (above) or fewer  
 45 (below) cases observed than expected. Teams are colored by contact level (legend). M refers to  
 46 men’s teams and W to women’s teams. **E.** The difference between the number of cases

47 observed and the number of cases expected (based on class size and scaled by the number of  
 48 cases expected; y axis) vs. the number of cases expected (x axis), per class year. The dashed  
 49 line at  $y = 0$  separates classes with more (above) or fewer (below) cases observed than  
 50 expected. Classes are colored by semester (legend).

### 51 Figure 3

52 Figure 3. Social connectivity network from the wifi co-location data identifies behavioral trends  
 53 that correlate with case counts

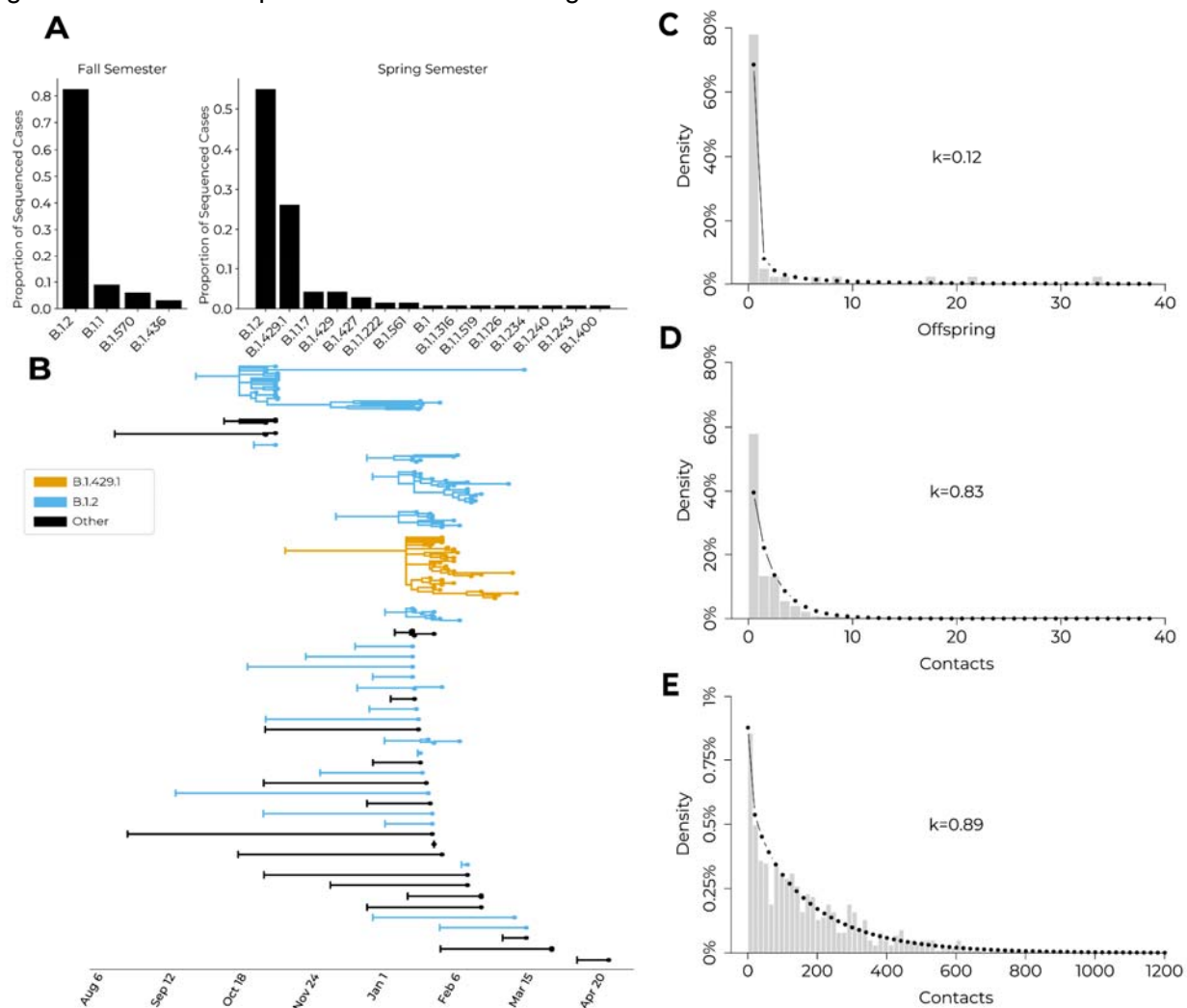


54 **A.** Left: Distributions of daily contacts (Appendix Table 11) for students who tested positive over  
 55 the course of each semester (orange) vs. those who remained negative (gray) over the course  
 56 of each semester. Effect sizes, 9.5 (Fall; positive median = 33.5, negative median = 24), 12.5  
 57 (Spring; positive median = 46.5, negative median = 34). Right: Distributions of average  
 58 exposure time per contact (Appendix Table 11), in minutes, for cases (orange) vs. those who  
 59 remained negative (gray). Effect sizes, 8.2 (Fall; positive median = 58, negative median = 49.8),  
 60 11.8 (Spring; positive median = 77, negative median = 58.8). **B.** Visual representation of the  
 61 network metric assortativity (AA; described in Supplemental Methods). We depict  
 62 network scenarios where the AA coefficient is equal to 1, 0, or -1. When AA = 1, pre-positive  
 63 individuals, defined as those within 10 days prior to their positive test, have interactions only  
 64 with pre-positive individuals, and vice versa. When AA = 0: pre-positives individuals have an  
 65 equal likelihood of interactions with pre-positive individuals and non-pre-positive individuals.  
 66 When AA = -1, pre-positive individuals have interactions only with non-pre-positive individuals,  
 67 and vice versa. Positive AA values indicate a higher propensity for within-group interactions,  
 68 while negative values indicate a higher propensity for between-group interactions. **C.**

70 Comparison of per-semester AA for individuals within a 10 day window of a positive test (*i.e.*,  
 71 pre-positives) vs. those who never tested positive (*i.e.*, negatives). 95% confidence intervals (CI;  
 72 blue) were calculated by permuting pre-positive and negative labels for individuals within the  
 73 proximity network each day, 40 times. The AA of the proximity network (black) was above the  
 74 upper bound of the CI for 69.4% (66/95 days) of the Fall 2020 semester, implying significance at  
 75  $p < 0.025$ . Only Fall 2020 is presented here; methodology and results were consistent for Spring  
 76 2021 (Appendix Figure 8). **D-E**. Comparison of smoothed case counts and smoothed AA for Fall  
 77 2020 (**D**) and Spring 2021 (**E**). Smoothing *via* the Savitzky-Golay filter (window length = 17,  
 78 polynomial order = 4).

## 79 Figure 4

80 Figure 4. Case clusters and lineages identified by viral genomic sequencing, and comparison of  
 81 genomic cases to reported social network degree distributions

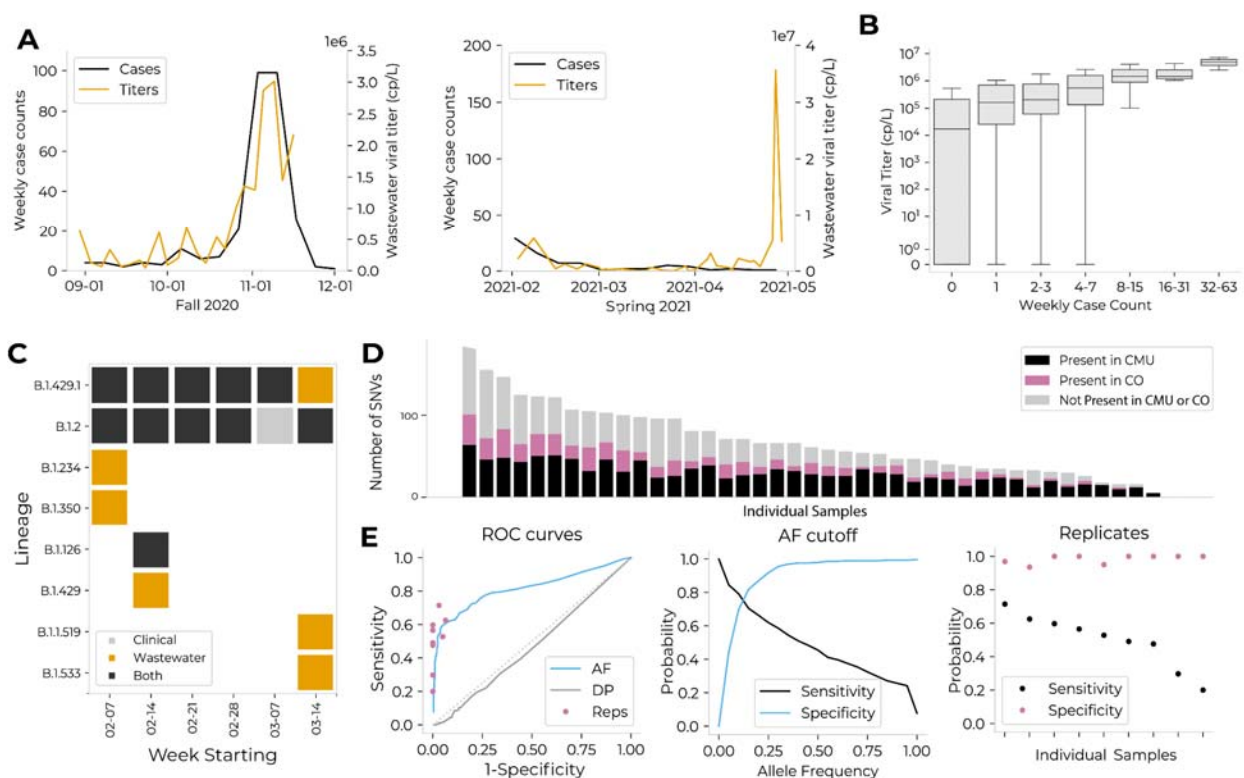


82 **A**. Pango lineage proportions for university cases during the Fall 2020 and Spring 2021  
 83 semesters. **B**. Phylogenetic trees for inferred introductions to the campus community with  
 84 branch lengths scaled to time. B.1.2 clusters (blue), the B.1.429.1 cluster (orange), and all other  
 85 lineages (black). Vertical bar on the left of each introduction indicates the inferred ancestral root  
 86

87 date of each university case or case cluster; cases are tip dots at right of each tree. **C.**  
 88 Distribution of offspring from phylogenetic clusters, with a negative binomial distribution fit and  
 89 overlaid (dotted line) to quantify overdispersion. Unique introductions and resulting offspring  
 90 were grouped into phylogenetic clusters; mean=2.56 offspring/introduction; k=0.13 (dispersion  
 91 parameter). **D.** Distribution of the number of contacts from positive individuals identified during  
 92 contact tracing, with a negative binomial distribution fit and overlaid (dotted line). Contacts were  
 93 defined as any individuals with interaction durations greater than 15 minutes in the 48-hour  
 94 period prior to positive test or symptom onset; mean=1.71 contacts per positive individual;  
 95 k=0.83. **E.** Distribution of the number of wifi contacts observed from positive individuals, with a  
 96 negative binomial distribution fit and overlaid (dotted line). Contacts were defined as individuals  
 97 with interaction durations greater than 15 minutes in the 48-hour period prior to testing positive  
 98 or symptom onset; mean=177.94 contacts per positive individual; k=0.89.

## 99 Figure 5

100 Figure 5. Wastewater surveillance and sequencing for measurement of aggregate viral load,  
 101 identification of circulating lineages, and comparison with viral genomes from contemporaneous  
 102 clinical cases

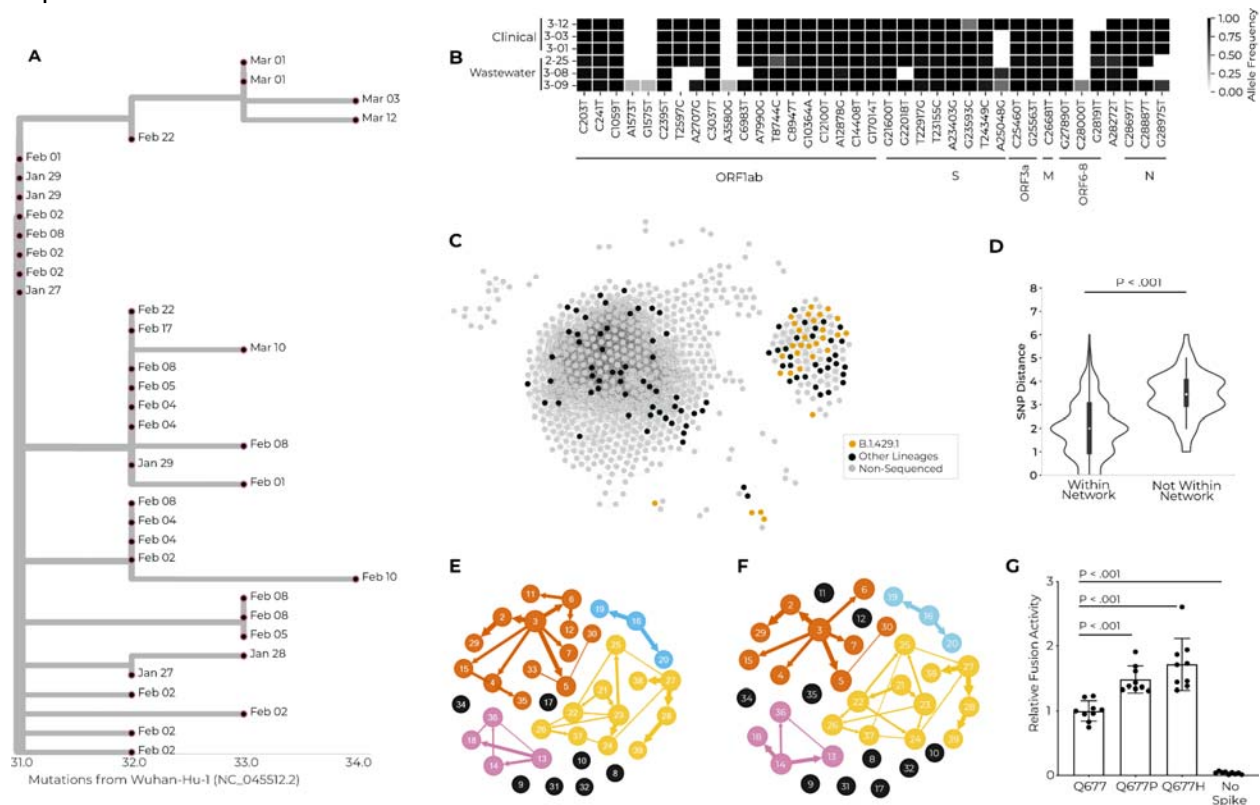


103 **A.** Average wastewater viral titers (orange) vs. weekly residential case count (black).  
 104 Residential case counts were calculated relative to the subsets of dorms monitored (75% of  
 105 residential population in Fall 2020; 99% in Spring 2021). There was an anomalous peak in  
 106 wastewater viral titer observed in April, which could be due to technical error, differential  
 107 shedding patterns, or undiscovered positive individuals. **B.** Viral titer (y axis) vs. binned weekly  
 108

109 case count (x axis; binned by powers of 2) for each wastewater sample. Viral titer and case  
 110 count were significantly associated *via* Fisher's exact test ( $p=0.04$ ) and Spearman's  
 111 correlation=0.40 ( $p<0.001$ ). **C.** Lineages detected on campus via wastewater or clinical  
 112 sequencing. **D.** The number of single nucleotide variants (SNVs) detected in wastewater  
 113 samples; each bar represents a single sample. Individual samples are organized on the x axis in  
 114 order of total number of SNVs. For each sample, SNVs are categorized by whether they were  
 115 present in clinical sequences from CMU (black), in clinical sequences from Colorado (pink), or in  
 116 neither (gray). On average, 51% of SNVs in a single wastewater sample were not found in CMU  
 117 clinical samples, and 36% were not found in Colorado clinical samples. **E.** Comparison of quality  
 118 control methods to remove SNVs not validated by presence in Colorado clinical sequences. The  
 119 three methods compared are: 1) allele frequency (AF), or discarding SNVs present at an allele  
 120 frequency below a given threshold; 2) read depth (DP), or discarding SNVs located at a site with  
 121 a read depth below a given threshold; and 3) replicates (Reps), or discarding SNVs not present  
 122 within both of two technical replicates of a given sample. These analyses are limited to the nine  
 123 samples for which technical replicates exist. Left: ROC curves for each of the three filters.  
 124 Middle: Sensitivity and specificity for allele frequency-based quality control method. Right:  
 125 Sensitivity and specificity for replicate-based quality control method.

## 126 Figure 6

127 Figure 6. A multimodal exploration of the novel lineage B.1.429.1 *via* clinical and environmental  
 128 genomic sequencing, wifi proximity analyses, transmission reconstruction networks, and  
 129 experimental validation

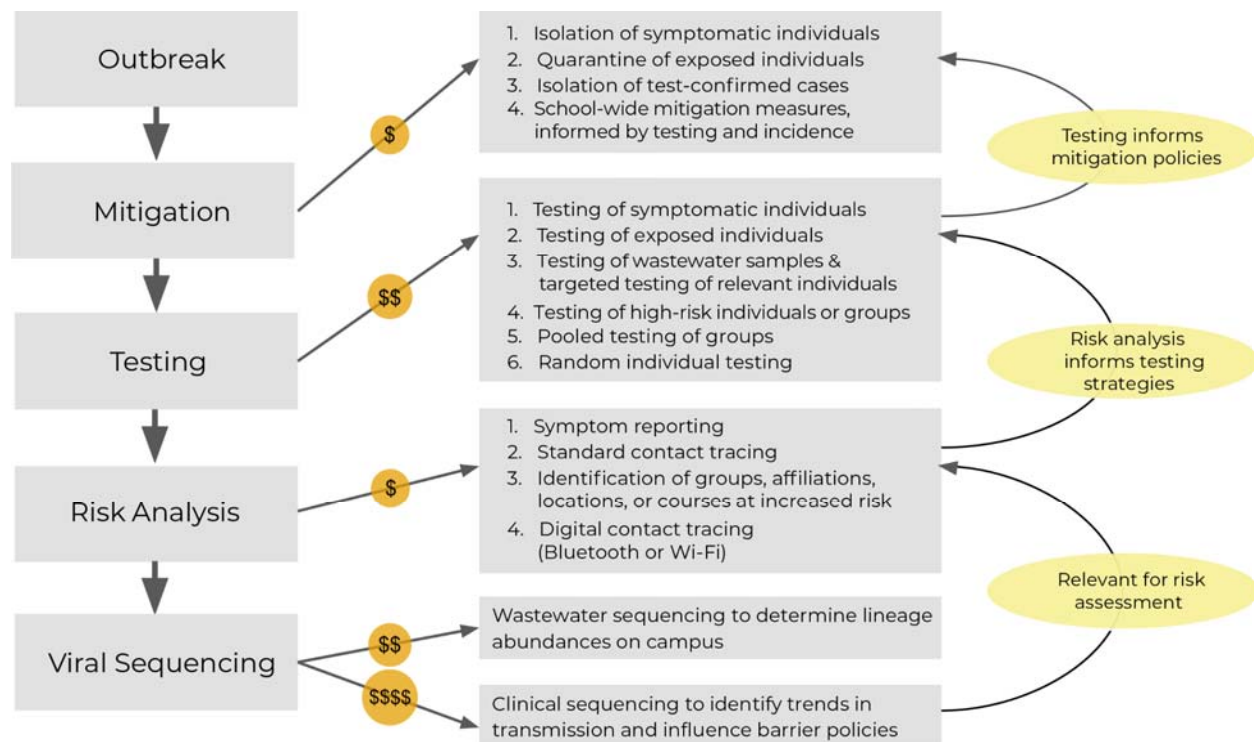




131 **A.** Phylogenetic tree showing the relationship between cases within the B.1.429.1 case cluster.  
132 Tree tips are anchored at their dates of sample collection, and branch lengths are scaled by  
133 maximum likelihood. One-to-many polytomies depict clonal amplification, with multiple cases  
134 with the same ancestral node rather than as a series of bifurcating branches. **B.** Three  
135 wastewater samples and three clinical samples (*y* axis), all of the B.1.429.1 lineage. The three  
136 wastewater samples had B.1.429.1 as the sole identified lineage, and were extracted from Site  
137 3, for which residential halls B and M are the only upstream contributors. Shown in comparison  
138 are clinical viral genomes from three students believed to have contributed effluent to these  
139 wastewater samples, based on residential status and test date. The *x* axis represents all single-  
140 nucleotide variants present in at least one wastewater sample with 25% allele frequency or  
141 greater. SNVs are grouped by genomic position. **C.** Social proximity network for interactions  
142 occurring between two individuals who are both within a 10-day window prior to testing positive.  
143 Edges in this network represent one or more simultaneous wifi access point connections. Each  
144 node represents a positive individual. The node color represents their sequencing status  
145 (legend). **D.** Comparison of genetic distance for individuals of the B.1.429.1 lineage who are or  
146 are not connected *via* the social proximity network shown in **(C)**. Effect size = 1 mutation. **E-F.**  
147 Transmission reconstruction network for B.1.429.1 cases created with genomic information as  
148 well as manual contact tracing data **(E)** or wifi-inferred 10-day contact data **(F)**. **G.** Results of  
149 cell-cell fusion activity of viral pseudotypes with the ancestral allele, or with the S:Q677P or  
150 S:Q677H amino acid changes, relative to a luminescent control with no Spike protein  
151 expressed.

## 152 **Figure 7**

153 Figure 7: A step-wise approach to outbreak surveillance with consideration for resource  
154 limitations

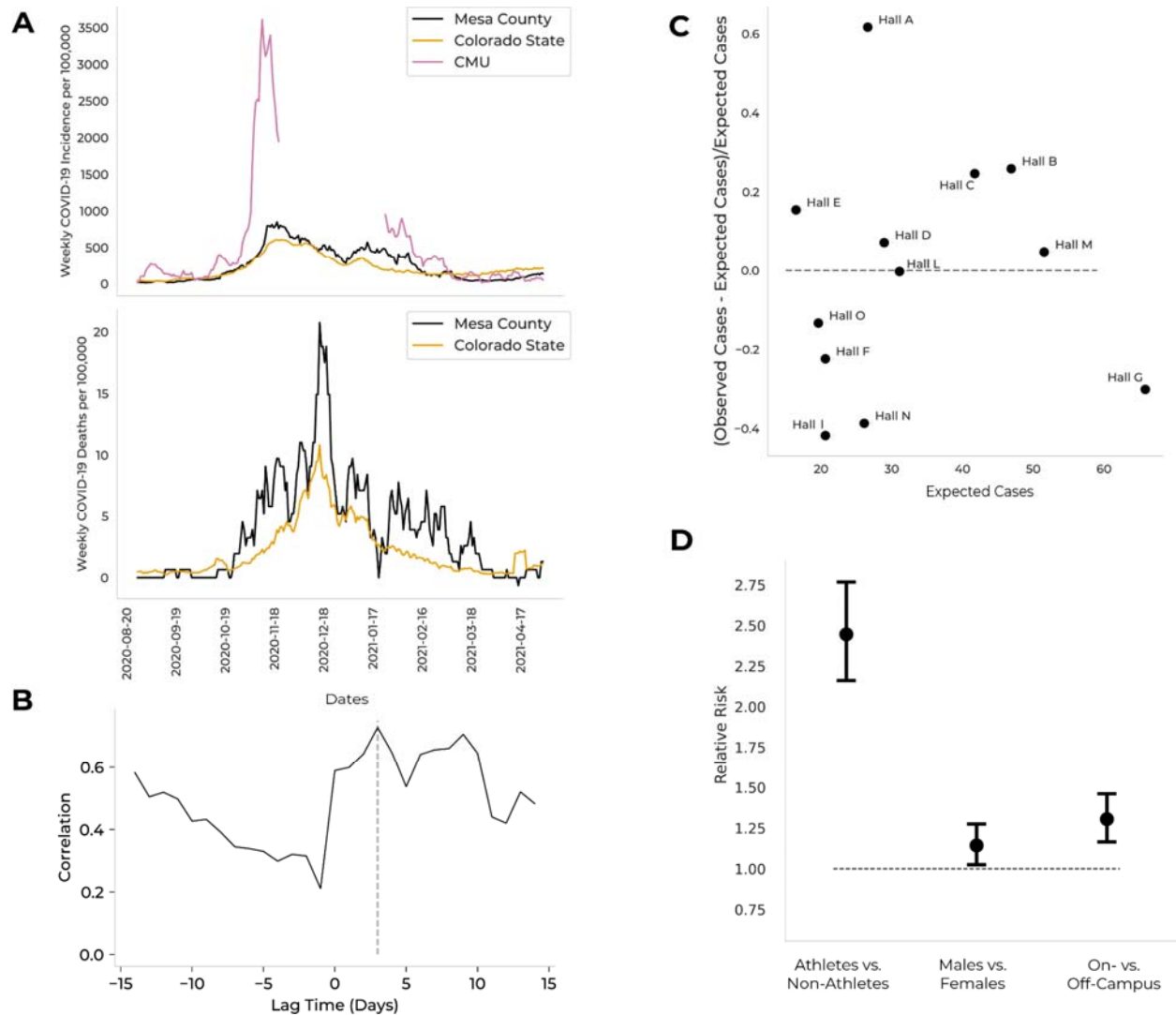


155  
156

157 Illustration of the flow of actions to employ during an institutional outbreak, with delineation of  
 158 relative cost and information feedback cycles. During an outbreak, initial mitigation measures  
 159 can be deployed prior to and independent of a surveillance program. A basic surveillance  
 160 program will first incorporate testing, the results of which will inform additional mitigation  
 161 policies. Next, analyses of case attributes can be used to assess the risk of infection for specific  
 162 sub-populations; these analyses will allow for development of specialized, directed testing  
 163 strategies. Finally, while more expensive, viral genomic sequencing of clinical or environmental  
 164 samples can be used to identify transmission trends and to detect emergent viral genomic  
 165 variation with potential public health or clinical relevance. This in turn can be used to inform  
 166 institutional policy and the intensity of mitigation efforts. Actions involving solely personnel time  
 167 are the least expensive to implement (*i.e.*, mitigation, risk analyses), while actions requiring both  
 168 personnel and laboratory consumables are more expensive (*i.e.*, testing), and actions requiring  
 169 laboratory consumables, highly trained personnel, and prolonged instrument time are most  
 170 expensive to implement (*i.e.*, viral sequencing).

## 171 Appendix Figure 1

172 Appendix Figure 1. Incidence rates at Colorado Mesa University (CMU), with surrounding areas  
 173 for context, and epidemiological risk factors for SARS-CoV-2 positivity at CMU

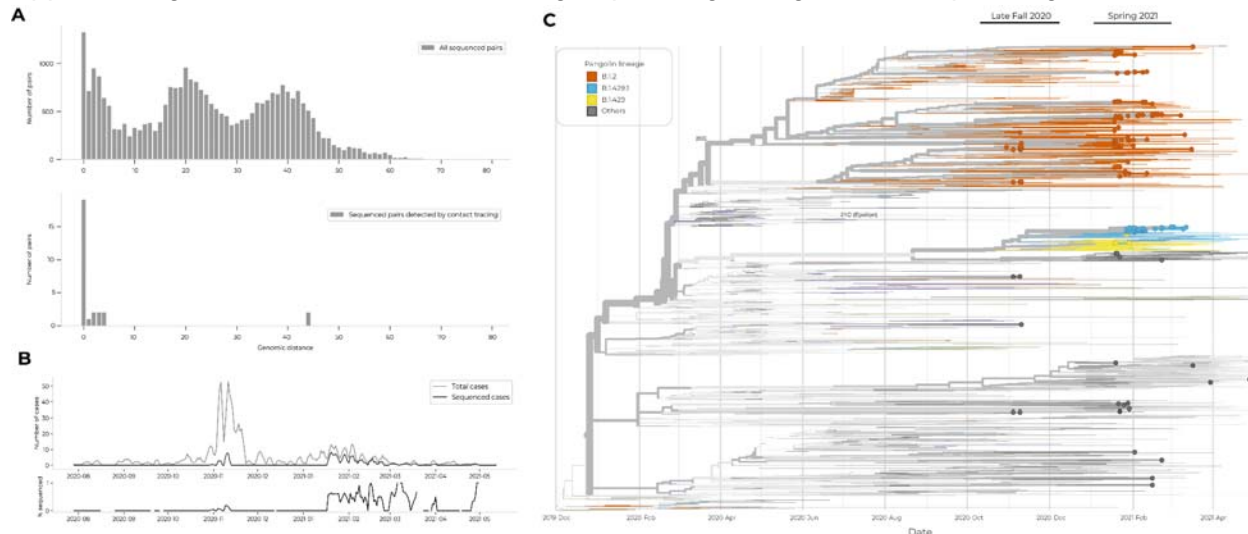


174  
 175 **A.** Weekly COVID-19 incidence at Colorado Mesa University (CMU; pink), in Mesa County  
 176 (black), and in Colorado (orange) over the 2020–2021 academic year (upper). Weekly COVID-  
 177 19 death rate in Mesa County (black) and in Colorado (orange) over the 2020–2021 academic  
 178 year (lower). Data from CMU were not analyzed from November 21–January 18 due to winter  
 179 recess. The correlations between CMU incidence rates and Mesa County incidence rates  
 180 (correlation = 0.73, lag = 3 days) and Mesa County death rates (correlation = 0.48, lag = 8 days)  
 181 were tested with lag times between -14 days (0 days for deaths) and 14 days, and the maximum  
 182 correlations and corresponding lag times are reported. **B.** The correlation between CMU  
 183 incidence rates and Mesa County incidence rates vs. the lag time. The dashed line at  $y = 3$   
 184 indicates the lag time that maximizes the cross-correlation. **C.** The difference between the  
 185 number of cases observed and the number of cases expected (given residence hall population  
 186 size and scaled by number of cases expected) vs. the number of cases expected, per residence  
 187 hall. The dashed line at  $y = 0$  separates halls with more (above) or fewer (below) cases  
 188 observed than expected. **D.** Relative risk (RR) of testing positive for COVID-19 given sports  
 189 team membership (athletes vs. non-athletes), sex (males vs. females), or residential status (on-  
 190 vs. off-campus). Circles represent the relative risk, with whiskers extending to the upper and

191 lower bounds of the 95% confidence interval. The dashed line at  $RR = 1$  represents the null  
192 hypothesis (*i.e.*, that there is no association between the risk factor and test positivity). An  $RR$   
193 greater than 1 implies that the first group listed (*i.e.*, athletes, males, or on-campus students)  
194 had a greater risk of testing positive than the second group listed (*i.e.*, non-athletes, females, or  
195 off-campus students).

## 196 Appendix Figure 2

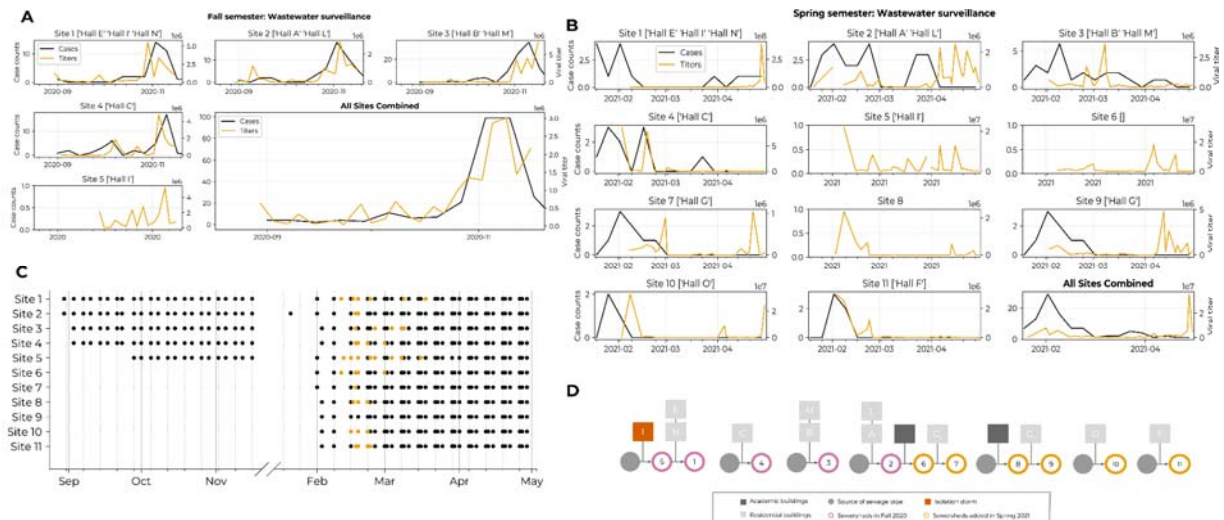
197 Appendix Figure 2. Detection of outbreak groups using viral genomic sequencing of cases



198 **A.** Distributions of genetic distance for all pairs of viral genomes (upper) and for pairs of viral  
199 genomes from positive individuals sharing interactions reported during contact tracing (lower).  
200 We sequenced viral samples from 18 pairs of positive individuals where one of the individuals  
201 identified the other as a close contact, and 11 pairs where both individuals identified one  
202 another as a close contact. Two outlier pairs had a genetic distance of 44 SNVs. In each of  
203 these pairs, an individual testing positive at the end of January 2021 had virus of the B.1.2  
204 lineage and indicated close contact with an individual who tested positive in early February (5-6  
205 days later) with virus of the B.1.429.1 lineage. **B.** Sequencing of positive cases via genomic  
206 surveillance across both semesters. Sequencing began October 2020, capturing cases  
207 associated with a Halloween-related outbreak. Shown are the total number of cases (top, thin  
208 line), total number of sequenced cases (top, bolded line), and percent of positive cases that  
209 were sequenced (bottom). **C.** Phylogenetic placement and temporal sampling of viral genomes  
210 sequenced from CMU clinical diagnostic tests. CMU nodes are depicted as dots among a global  
211 tree of contextual sequences, weighted toward sequences collected from Colorado and  
212 surrounding states, but including uniformly-sampled genomes from all dates and geographic  
213 regions, as well as genomes close in genetic distance to CMU sequences. Interactive version  
214 available at <https://auspice.broadinstitute.org>.  
215

## 216 Appendix Figure 3

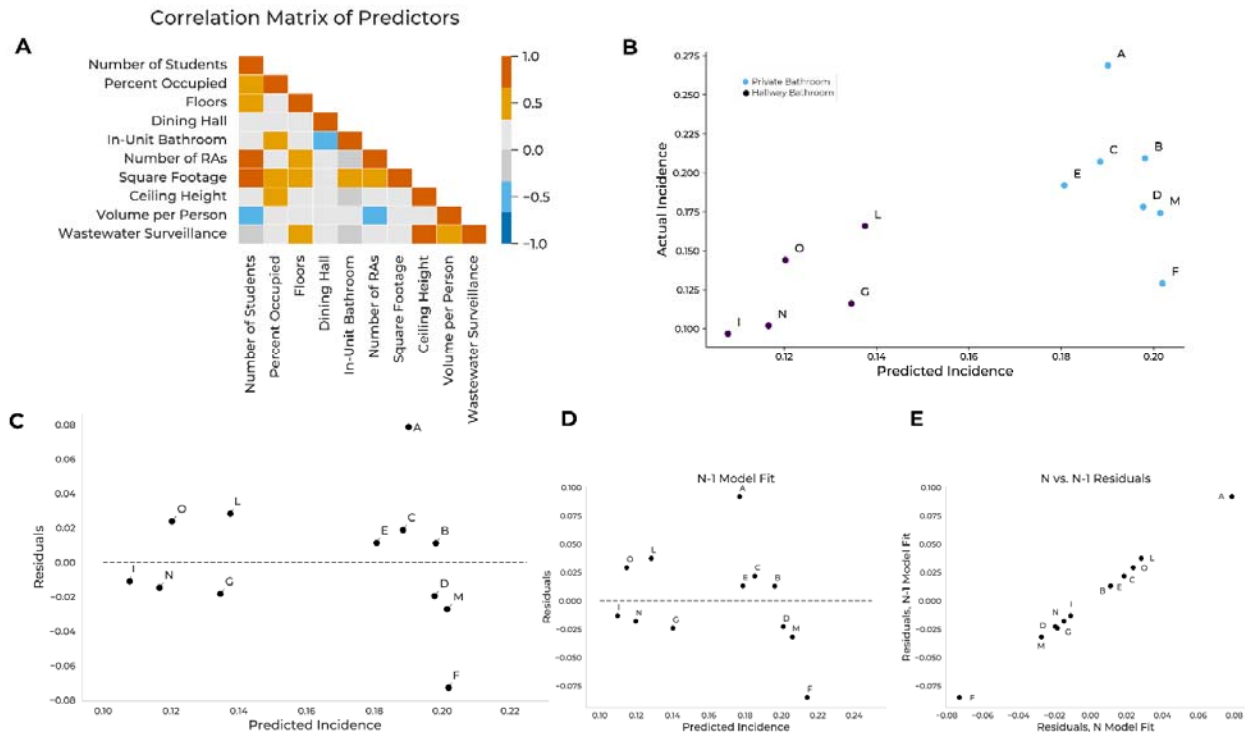
217 Appendix Figure 3. Summary of wastewater surveillance implemented at Colorado Mesa  
218 University across Fall 2020 and Spring 2021



219  
 220 **A-B.** Comparison of wastewater viral titer (orange) and weekly case count (black) for each  
 221 wastewater site in the Fall semester (**A**) and Spring semester (**B**). **C.** Sample collection  
 222 frequency for wastewater surveillance in the 2020–2021 academic year. Wastewater samples  
 223 were collected twice weekly in the Fall across 5 sites, and three times weekly in the Spring  
 224 across 11 sites. Each dot represents an independent collection event, with dots shown in  
 225 orange representing sequenced wastewater samples. **D.** Schematic showing which residential  
 226 or academic buildings (squares) contributed effluent to each monitored wastewater site (circles).  
 227 Residence hall I (red square) housed a small number of students who had tested positive and  
 228 were in isolation. Wastewater sites are represented by circles, with filled-in gray circles  
 229 representing sites utilized to collect baseline measurements where there were no upstream  
 230 contributors to that particular sewage system. Sites shown in pink were added in Fall 2020 and  
 231 remained in use into Spring 2021, while sites shown in orange were added in Spring 2021.

## 232 Appendix Figure 4

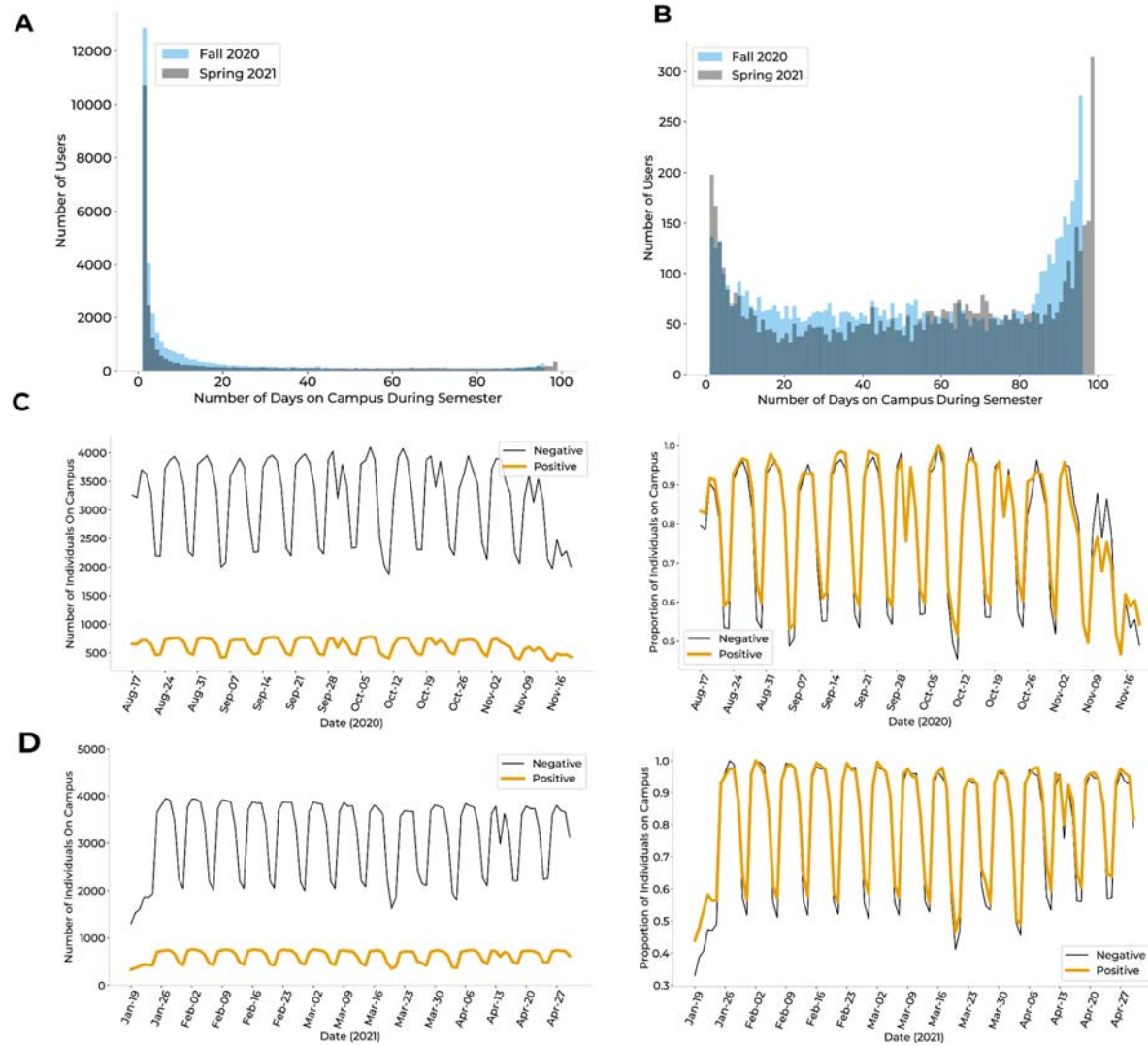
233 Appendix Figure 4. Predictions of COVID-19 incidence rates in Colorado Mesa University  
 234 residence halls *via* a linear regression model



235  
 236 **A.** Descriptive attributes of residence halls, including number of students, percent occupied  
 237 (number of available beds / number of students), number of floors, the presence of a meal plan  
 238 requirement ('dining hall'), the presence of an in-unit bathroom ('private bath'), the number of  
 239 resident advisors (RAs), square footage, ceiling height, volume per person, and the presence of  
 240 wastewater surveillance, were used as predictors in the regression model. Non-zero correlation  
 241 coefficients between pairs of predictive variables indicate multicollinearity. **B.** Observed  
 242 incidence rates vs. predicted incidence rates, by residence hall. Predictions come from the  
 243 model that minimized the Akaike and Bayesian Information Criteria. Colors indicate the  
 244 difference in predicted incidence associated with a private vs. a hallway bathroom. **C.** Residuals  
 245 vs. predicted incidence rates, by residence hall. Root-mean-square-error = 3.6%. **D.** Residuals  
 246 vs. predicted incidence rates, from leave-one-out cross-validation, by residence hall. Leave-one-  
 247 out cross-validation (*i.e.*,  $N-1$  model fit, where  $N$  = number of residence halls) was conducted  
 248 such that each hall's incidence rate was predicted *via* a linear model whose coefficients were  
 249 determined with training data from all other halls. Root-mean-square-error = 4.2%. **E.** Residuals  
 250 from the leave-one-out cross-validation ( $N-1$  model fit) vs. residuals from the full model ( $N$   
 251 model fit).

## 252 Appendix Figure 5

253 Appendix Figure 5. On-campus presence, as inferred by wifi proximity data, by semester and by  
 254 user category

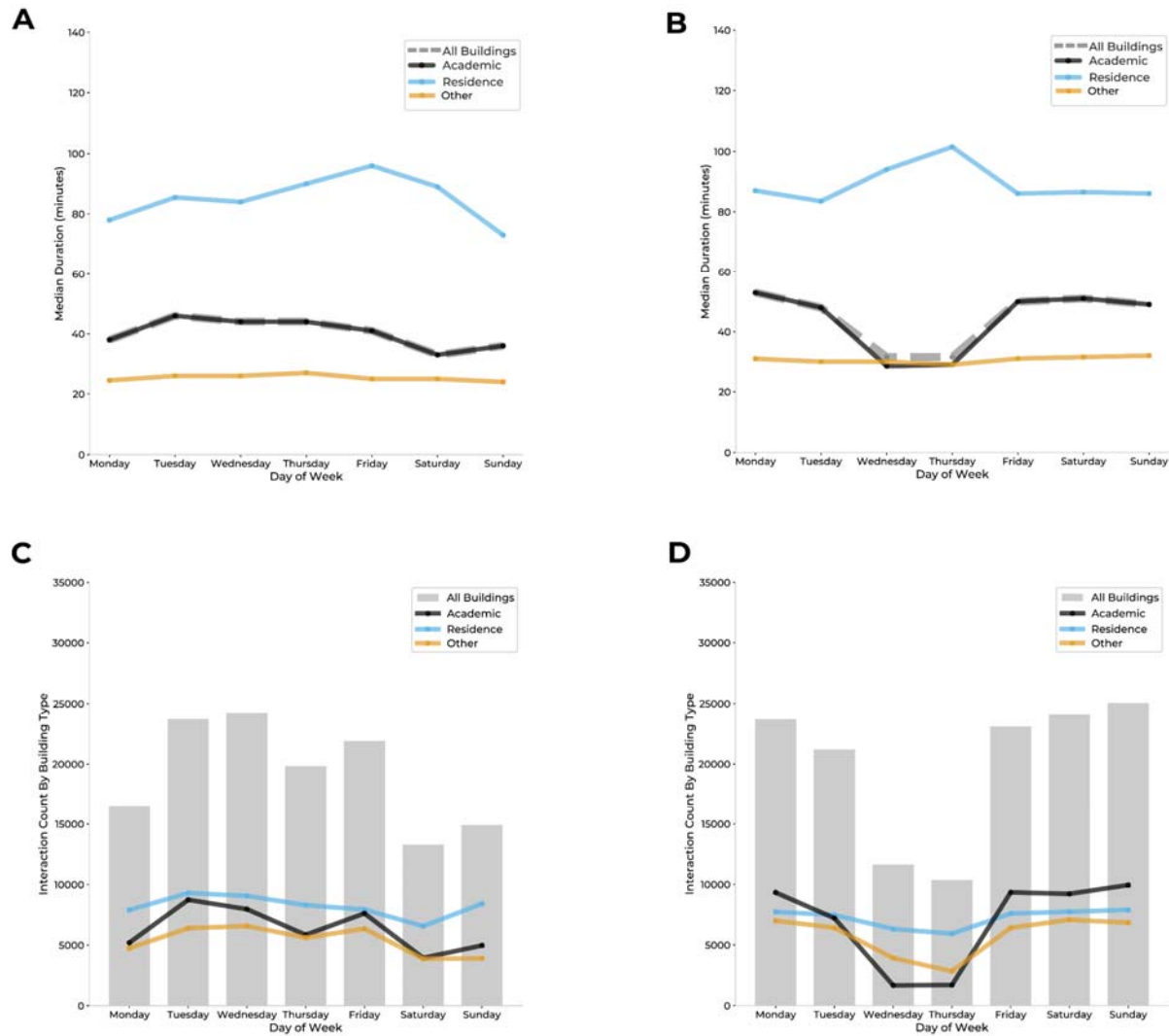


255  
256  
257  
258  
259  
260  
261  
262  
263  
264  
265  
266  
267  
268  
269

**A.** Distribution of the number of days present on campus for all users found in the wifi network, colored by semester. **B.** Distribution of the number of days present on campus for all users found in the wifi network after removal of unauthenticated users, non-students, and infrequent users, colored by semester. This cleaned wifi proximity network was used for all future analyses. **C.** Number (left) and proportion (right) of positive students (orange) and negative students (black) on campus by day for Fall 2020 (Appendix Table 11). There was no significant difference in the proportion distributions ( $p = 0.282$ ). We found a significant correlation in the trends of the proportion distributions (Pearson Correlation: .976,  $p < .0001$ ). **D.** Number (left) and proportion (right) of positive students (orange) and negative students (black) on campus by day for Spring 2021 (Appendix Table 11). There was no significant difference in the proportion distributions ( $p = 0.248$ ). We found a significant correlation in the trends of the proportion distributions (Pearson Correlation: .99,  $p < .0001$ ).

270 **Appendix Figure 6**

271 Appendix Figure 6. Wifi network access patterns by building and by semester.

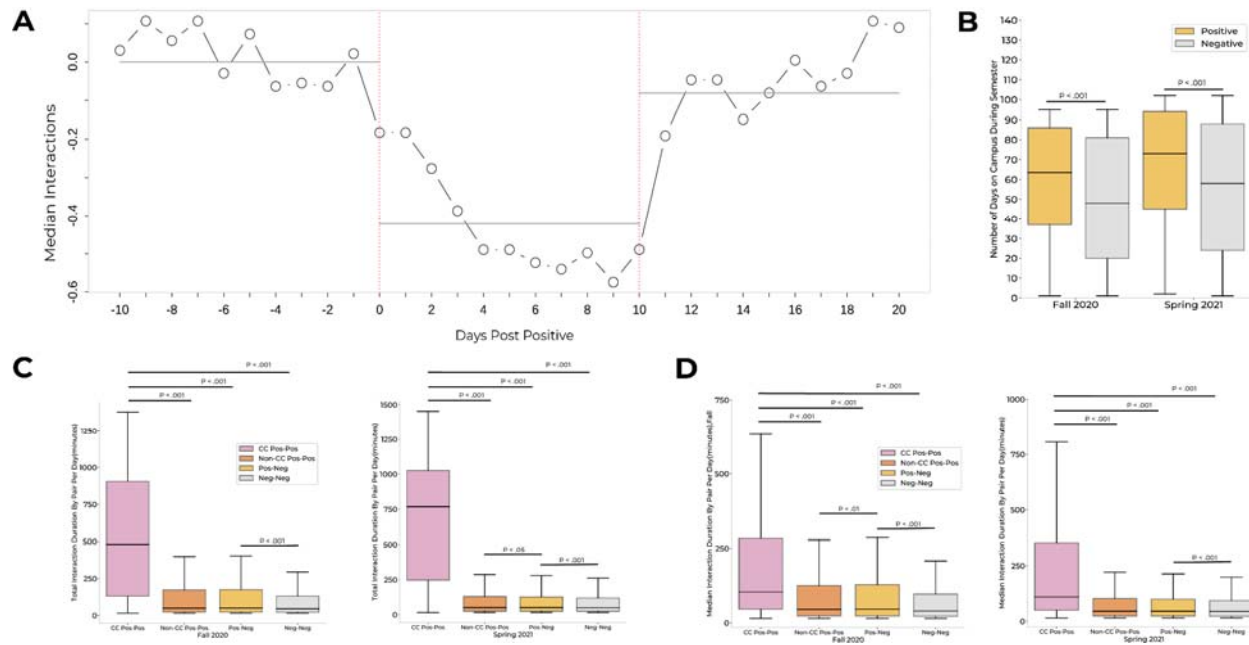


272  
 273 **A-B.** Median duration of access point connections in minutes, per day of the week and by  
 274 building type (academic, residential, other, or all buildings) for Fall 2020 (**A**) and Spring 2021 (**B**;  
 275 Appendix Table 11). **C-D.** Daily number of AP connections, per day of the week and by building  
 276 type (academic, residential, other, or all buildings) for Fall 2020 (**C**) and Spring 2021 (**D**;  
 277 Appendix Table 11).

278 **Appendix Figure 7**

279 Appendix Figure 7. Interaction patterns of individuals and of pairs of individuals by testing status  
 280

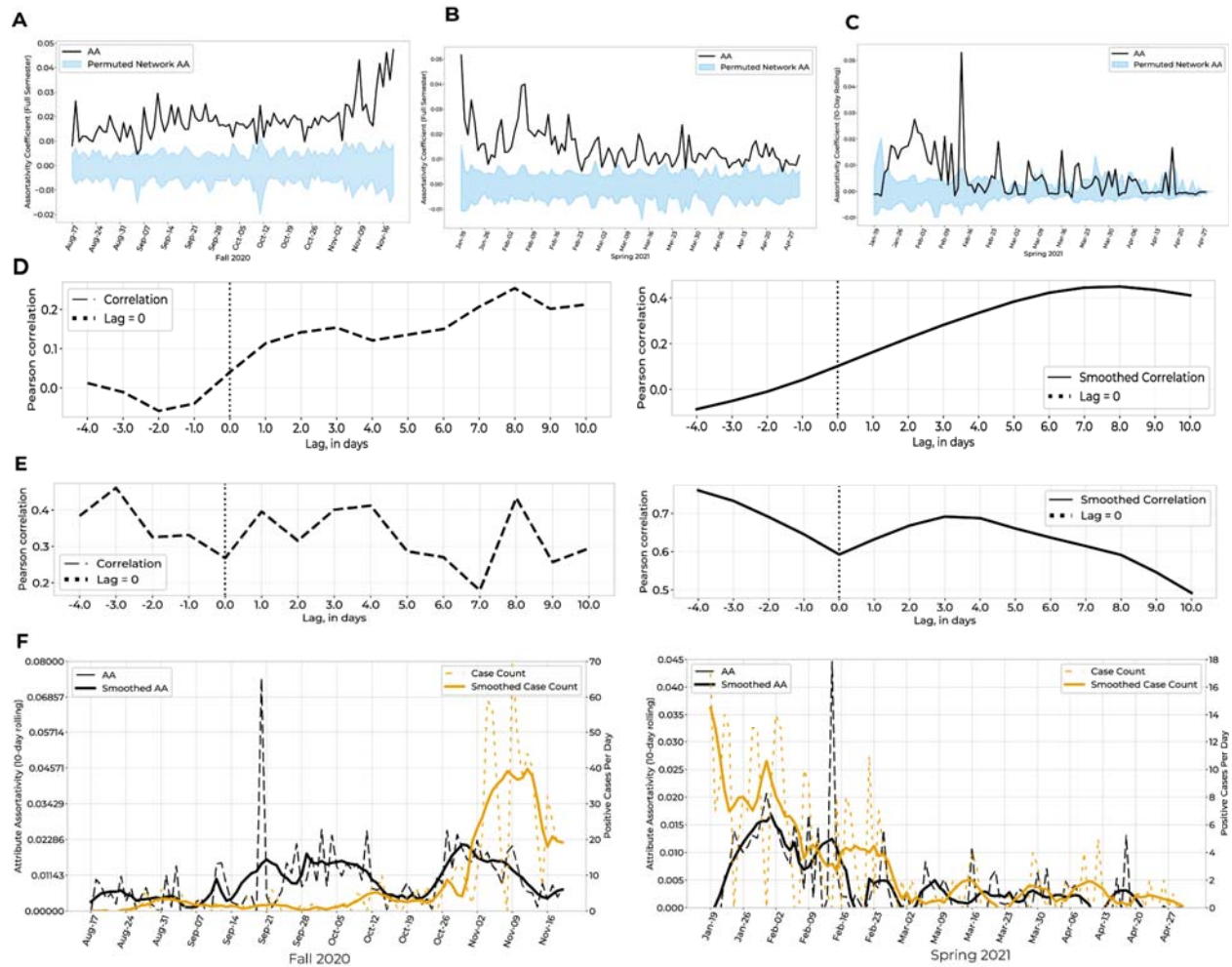




281  
 282 **A.** Median number of wifi contacts per day for the 30-day period surrounding the isolation period  
 283 of positive cases. Day 0 was calculated as the earliest of symptom onset date and test date.  
 284 Black lines indicate the median number of contacts (y-axis) per individual for every day across  
 285 the period (x-axis). **B.** The number of days on campus for positive (orange) vs. negative (gray)  
 286 individuals. Effect sizes, 15 days (median positive: 66; median negative: 51; Fall 2020) and 16  
 287 days (median positive: 76; median negative: 60; Spring 2021). Gray bars indicate averages for  
 288 three 10-day periods: pre-isolation, isolation, and post-isolation. **C.** Distributions of total pairwise  
 289 daily interaction duration, for pairings categorized by testing status: CC Pos-Pos, pairs of pre-  
 290 positive individuals with an association reported in manual contact tracing; Non-CC Pos-Pos,  
 291 pairs of pre-positive individuals without an association reported in manual contact tracing; Pos-  
 292 Neg, pairs of one pre-positive and one negative individual; Neg-Neg, pairs of two negative  
 293 individuals. Pre-positive individuals were defined as students within the 10-day window prior to  
 294 testing positive. **D.** Distributions of median interaction duration by pair per day, for pairings  
 295 categorized by test status (see above description). Positive individuals were defined as students  
 296 within the 10-day window prior to testing positive. See Appendix Table 11 for equations used in  
 297 panels **A**, **C**, and **D**.

## 298 Appendix Figure 8

299 Appendix Figure 8. Comparison of randomness vs true assortativity within the wifi proximity  
 300 network in conjunction with semester daily case counts



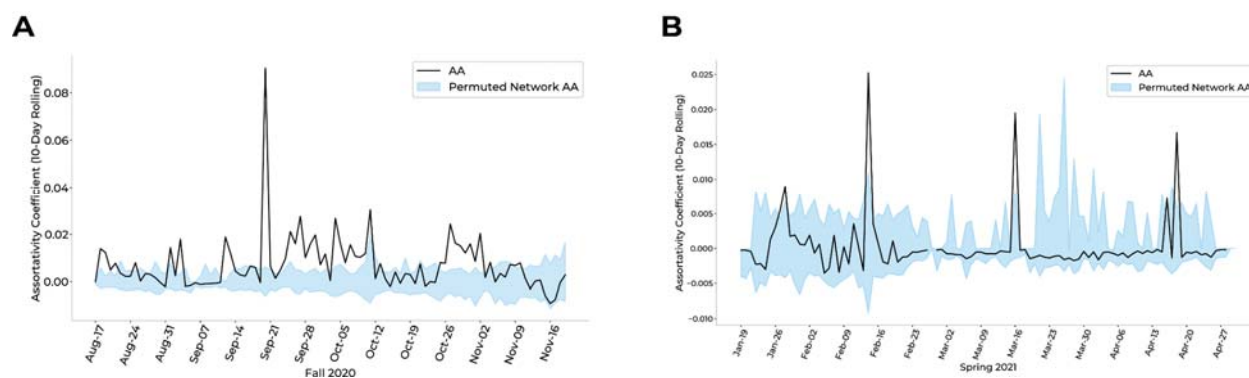
301  
 302 **A-B.** Comparison of attribute assortativity (AA) for positives vs. negatives, for Fall 2020 (**A**) and  
 303 Spring 2021 (**B**). 95% Confidence Intervals (CI; blue) were calculated by permuting positive and  
 304 negative labels for individuals within the proximity network each day. The AA of the proximity  
 305 network (black) was above the upper bound of the CI for 98.9% (94/95 days) in the Fall 2020  
 306 semester and 98%(100/102 days) in the Spring 2021 semester, indicating significance with  $p <$   
 307 0.025. **C.** We calculated the same metric with altered groupings: pre-positives (all individuals  
 308 within a 10-day window prior to their positive test) vs. negatives (individuals not within a 10-day  
 309 window prior to a positive test, regardless of overall semester testing status). The AA of the  
 310 proximity network (black) was above the upper bound of the CI for 37.2% (38/102 days) in the  
 311 Spring 2021 semester, indicating significance with  $p <$  0.025. **D.** Correlations between daily AA  
 312 (pre-positives vs. negatives) and daily case count with varying lag times, where both AA and  
 313 case count are non-smoothed (top) or smoothed using Savitzky Golay filter (bottom), for Fall  
 314 2020. The highest correlation occurs with a lag time such that AA preceded the case count by 8  
 315 days (Pearson correlation = 0.253 for non-smoothed, 0.449 for smoothed). **E.** Cross-  
 316 correlations between daily AA (pre-positives vs. negatives) and daily case count with varying lag  
 317 times, where both AA and case count are non-smoothed (top) or smoothed using Savitzky  
 318 Golay filter (bottom), for Spring 2021. The highest correlation occurs with lag time such that AA  
 319 preceded the case count by 4 days (Pearson correlation=0.411 for non-smoothed; 3 days for

320 smoothed, with correlation = 0.691). **F.** Unsmoothed case counts and unsmoothed AA vs.  
321 smoothed case counts and smoothed AA for Fall 2020 (left) and Spring 2021 (right).

## 322 Appendix Figure 9

323 Appendix Figure 9. Comparison of assortativity within the wifi proximity network when defining  
324 the “pre-positive” attribute as positive individuals without pairwise associations within the contact  
325 tracing data.

326



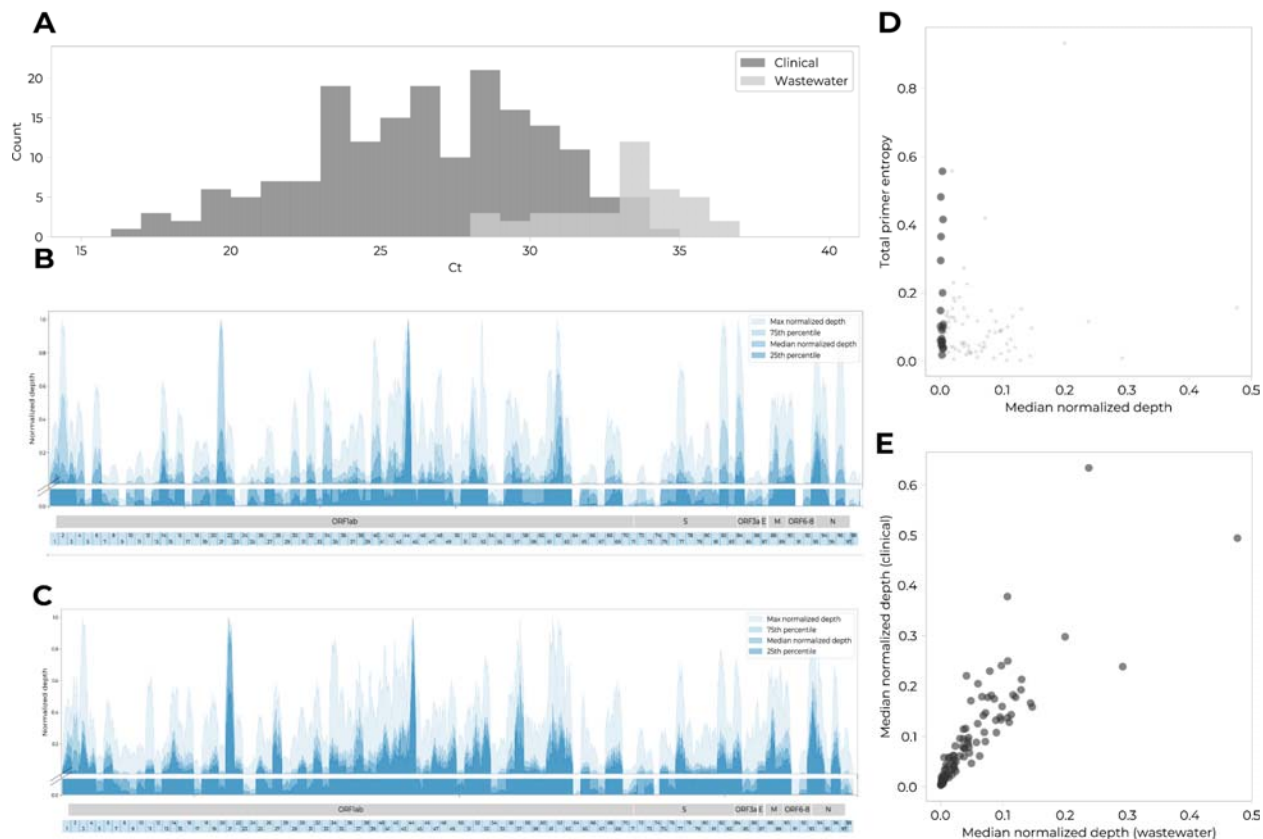
327

328

329 **A-B.** Comparison of attribute assortativity (AA) for pre-positives vs. negatives, for Fall 2020 (**A**)  
330 and Spring 2021 (**B**). 95% Confidence Intervals (CI; blue) were calculated by permuting pre-  
331 positive and negative labels for individuals within the proximity network each day. We calculated  
332 the same metric with pre-positives defined as individuals within a 10-day window prior to their  
333 positive test without pairwise associations with other pre-positive individuals in the contact  
334 tracing data and negatives defined as individuals not within a 10-day window prior to a positive  
335 test, regardless of overall semester testing status. The AA of the proximity network (black) was  
336 above the upper bound of the CI for 45.2% (43/95 days) of the Fall 2020 semester (**A**) and 8.8%  
337 (9/102 days) of the Spring 2021 semester (**B**), indicating significance with  $p < 0.025$ .

## 338 Appendix Figure 10

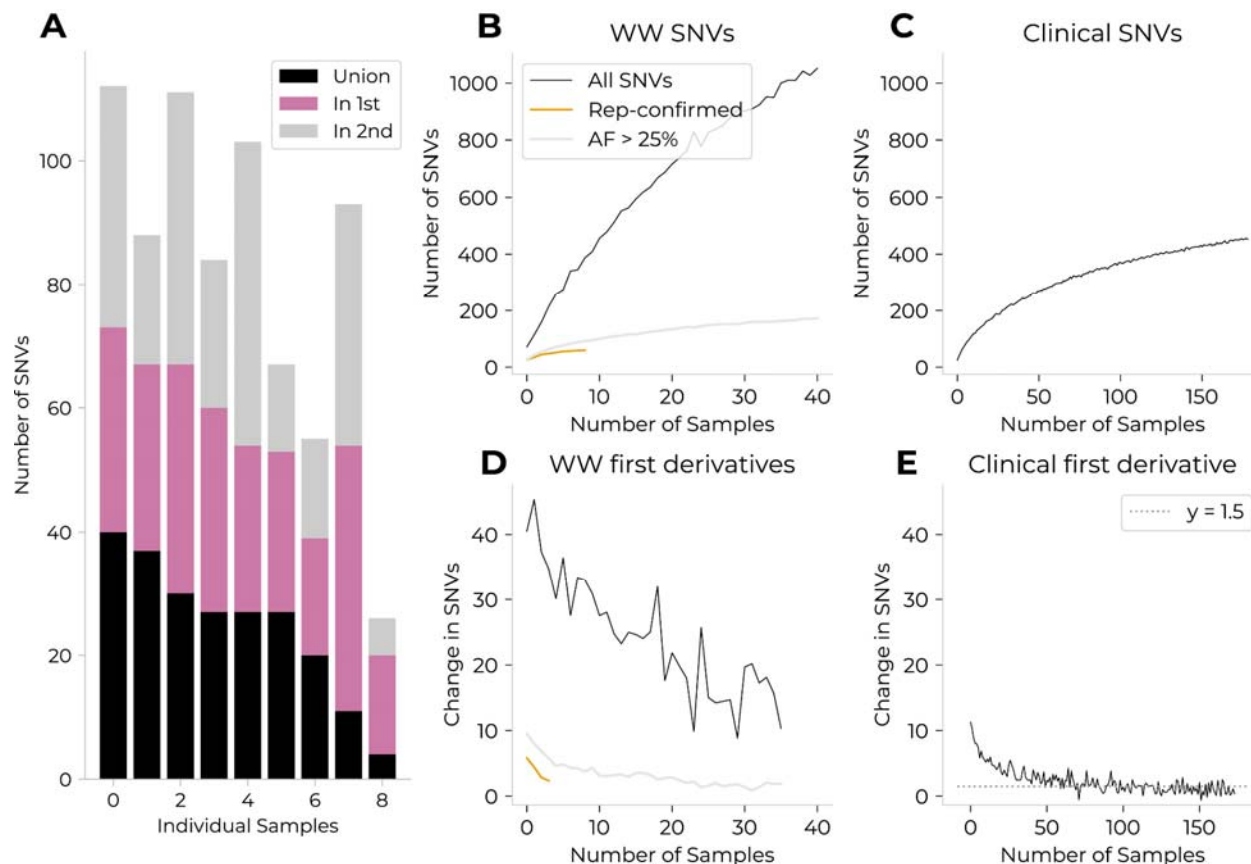
339 Appendix Figure 10. Sequenced wastewater samples, though subject to increased degradation,  
340 are of similar genome coverage as sequenced clinical samples



341  
342 **A.** Cycle thresholds (Ct) for sequenced wastewater and clinical samples from Colorado Mesa  
343 University. **B-C.** Median normalized read depth per base, across all wastewater (**B**) and clinical  
344 (**C**) samples. The coloring indicates quartiles across all wastewater or clinical samples. Regions  
345 of lower depth in wastewater sequencing are of similarly low depth in clinical sequencing. **D.**  
346 Comparison of average amplicon read depth (x axis) and average amplicon primer entropy (y  
347 axis) for wastewater samples. We found no correlation between amplicon read depth and  
348 primer entropy (Pearson correlation coefficient of  $r = .02$ ,  $p = 0.81$ ). The 20 amplicons with  
349 lowest median normalized depth are shown as larger circles. **E.** Comparison of median  
350 normalized depth per amplicon between wastewater (x axis) and clinical (y axis) samples. There  
351 is a linear correlation between corresponding amplicons (Pearson correlation coefficient of  $r =$   
352  $0.86$ ;  $p < 0.001$ ).

## 353 Appendix Figure 11

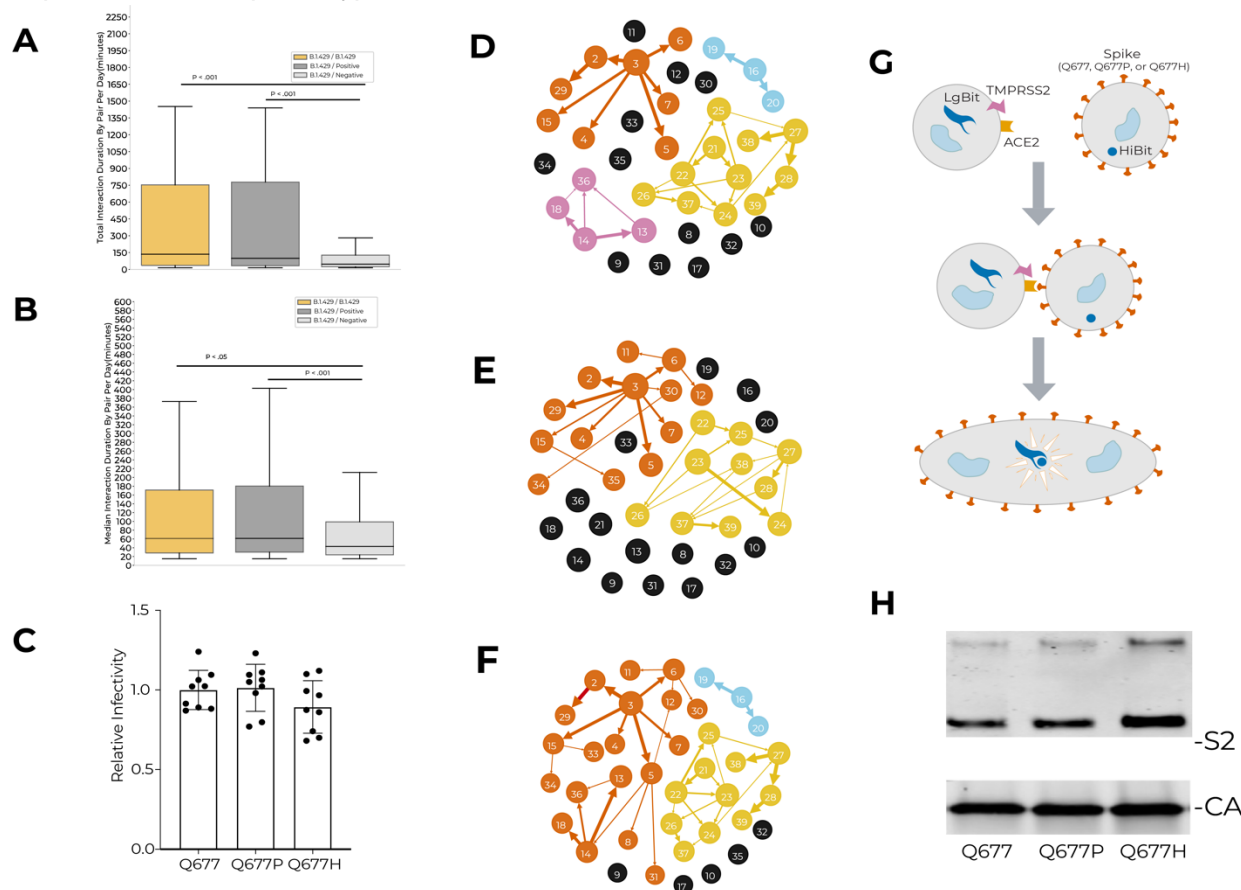
354 Appendix Figure 11. Presence of previously undetected mutations in sequenced wastewater  
355 samples suggests sequencing error



356  
357 **A.** Distribution of single-nucleotide variants (SNVs) that were present in only one technical  
358 duplicate (pink and gray) or in both duplicates (black). The samples are ordered relative to the  
359 number of replicate-confirmed SNVs. **B.** Predictions for the number of unique SNVs that can be  
360 expected for a given number of wastewater samples, calculated per the methodology described  
361 in the Supplemental Methods. We additionally calculated the number of unique SNVs that would  
362 be expected to pass an allele frequency quality control threshold of 25% (gray) or to be seen in  
363 at least both technical replicates of any given sample (orange). **C.** Predictions for the number of  
364 unique consensus-level SNVs that can be expected for a given number of clinical samples,  
365 calculated per the methodology described in the Supplemental Methods. **D.** Smoothed  
366 (window=5) first derivative of unique wastewater SNVs per sample. Legend is the same as in  
367 panel (B). This highlights that while the first derivatives for both replicate-confirmed SNVs  
368 (orange) and SNVs with an allele frequency greater than 25% (gray) approaches a rate of 1-3  
369 new SNVs per sample, the first derivative for all SNVs of any allele frequency (black)  
370 approaches a rate of >10 new SNVs per sample. **E.** Smoothed (window=5) first derivative of  
371 unique clinical consensus-level SNVs per sample. This highlights that the first derivative for all  
372 consensus-level SNVs seen in clinical samples approaches a rate of 1.5 new SNVs per sample.  
373 The comparison between (D) and (E) lends support to the hypothesis that most SNVs seen in  
374 wastewater samples are spurious, and that either confirming SNVs via technical replicates or a  
375 high allele frequency threshold is sufficient to remove most spurious SNVs.

## 376 Appendix Figure 12

377 Appendix Figure 12. Social proximity patterns, transmission reconstruction networks, and  
378 experimental viral phenotypes associated with B.1.429.1



379  
380 **A.** Distributions of total daily interaction duration (Appendix Table 11), per pair and per day, for  
381 pairs of B.1.429.1-positive (within 10 days of positive tests), non-B.1.429.1-positive (within 10  
382 days of positive tests), and negative individuals. Non-B.1.429.1-positive individuals are defined  
383 as positive individuals whose viral genome was not sequenced or was sequenced and  
384 determined not to be B.1.429.1. **B.** Distributions of median daily interaction duration (Appendix  
385 Table 11), per pair per day, for pairs of B.1.429.1-positive (within 10 days of positive tests), non-  
386 B.1.429.1-positive (within 10 days of positive tests), and negative individuals. **C.** Results of  
387 infectivity of viral pseudotypes with the ancestral allele, or with the S:Q677P or S:Q677H amino  
388 acid changes, relative to a luminescent control with no Spike protein expressed. **D-F.**  
389 Transmission reconstruction network for B.429.1 cases created with solely genomic information  
390 (**D**), solely manual contact tracing data (**E**), and both genomic information and wifi-inferred 2-  
391 day contact data (**F**). **G.** Conceptual diagram showing the experimental strategy for assessing  
392 the fusogenicity of the S:Q677H or S:Q677P amino acid changes relative to the ancestral  
393 residue, using two populations of cells: one expressing the modified Spike protein on the cell  
394 surface, and a second expressing the ACE2/TMPRSS2 receptors. The two populations were  
395 combined and fusion signal was assessed via HiBit-LgBit luminescent reporter. **H.** Western blot  
396 illustrating successful creation of viral pseudotype particles bearing Spike protein with S:677Q,  
397 S:Q677H, and S:Q677P.

398 **Appendix Table 1**

399 Appendix Table 1. Properties of residence halls at Colorado Mesa University

400

| Hall   | Number of Students | Percent Occupancy | Number of Floors | Dining Hall Requirement | In-unit Bathroom | Number of RAs | Square Footage | Ceiling Height | Volume per Person | Number of COVID-19 Cases |
|--------|--------------------|-------------------|------------------|-------------------------|------------------|---------------|----------------|----------------|-------------------|--------------------------|
| Hall A | 160                | 0.89              | 3                | 1                       | 1                | 5             | 46695          | 8              | 2334.75           | 43                       |
| Hall B | 282                | 0.94              | 4                | 1                       | 1                | 4             | 96429          | 8              | 2735.57           | 59                       |
| Hall C | 251                | 0.88              | 4                | 1                       | 1                | 8             | 80100          | 8              | 2552.99           | 52                       |
| Hall D | 174                | 0.94              | 4                | 0                       | 1                | 6             | 59360          | 8              | 2729.12           | 31                       |
| Hall E | 99                 | 0.83              | 3                | 0                       | 1                | 4             | 28080          | 8              | 2269.09           | 19                       |
| Hall F | 124                | 0.97              | 4                | 1                       | 1                | 5             | 45996          | 9.67           | 3586.95           | 16                       |
| Hall G | 396                | 0.91              | 4.25             | 1                       | 0                | 15            | 93650          | 9.67           | 2286.86           | 46                       |
| Hall I | 124                | 0.73              | 3                | 1                       | 0                | 4             | 42507          | 8              | 2742.39           | 12                       |
| Hall L | 187                | 0.93              | 3                | 1                       | 0                | 6             | 42883          | 8              | 1834.57           | 31                       |
| Hall M | 310                | 0.97              | 5                | 1                       | 1                | 10            | 72500          | 8              | 1870.97           | 54                       |
| Hall N | 157                | 0.79              | 3                | 1                       | 0                | 6             | 44178          | 8              | 2251.11           | 16                       |
| Hall O | 118                | 0.81              | 5                | 1                       | 0                | 5             | 43843          | 8              | 2972.41           | 17                       |

401

402 Structural and communal properties of residence halls. Volume per person was calculated as  
 403 square footage \* ceiling height / number of students per hall and serves as a proxy for air  
 404 volume per person. Hall G has 4 floors and a partial basement, covering approximately 25% of  
 405 the square footage of the other floors.

406 **Appendix Table 2**

407 Appendix Table 2. Properties of athletic teams at Colorado Mesa University

408

| Team                    | Number of Students | Contact Level | Season | Location | Number of COVID-19 Cases |
|-------------------------|--------------------|---------------|--------|----------|--------------------------|
| Women's Golf            | 11                 | Low           | both   | outdoor  | <5                       |
| Women's Club Volleyball | 11                 | Low           | both   | indoor   | <5                       |
| Men's Golf              | 12                 | Low           | both   | outdoor  | <5                       |
| Women's Tennis          | 12                 | Low           | both   | outdoor  | <5                       |
| Women's Cross Country   | 14                 | Low           | fall   | outdoor  | <5                       |
| Men's Triathlon         | 18                 | Low           | both   | outdoor  | <5                       |
| Cycling                 | 65                 | Low           | both   | outdoor  | <5                       |
| Women's Swimming        | 33                 | Low           | both   | indoor   | 6                        |

|                    |    |          |        |         |    |
|--------------------|----|----------|--------|---------|----|
| Men's Tennis       | 10 | Low      | both   | outdoor | 7  |
| Women's Triathlon  | 14 | Low      | both   | outdoor | 7  |
| Cheerleading       | 30 | Moderate | both   | indoor  | 7  |
| Men's Soccer       | 30 | High     | fall   | outdoor | 8  |
| Sand Volleyball    | 19 | Moderate | spring | outdoor | 8  |
| Women's Basketball | 15 | High     | both   | indoor  | 9  |
| Women's Wrestling  | 22 | High     | both   | indoor  | 9  |
| Indoor Volleyball  | 20 | Moderate | fall   | indoor  | 9  |
| Men's Track        | 55 | Moderate | both   | both    | 10 |
| Men's Basketball   | 19 | High     | both   | indoor  | 11 |
| Men's Swimming     | 38 | Low      | both   | indoor  | 11 |
| Women's Lacrosse   | 30 | Moderate | spring | outdoor | 12 |
| Women's Soccer     | 35 | High     | fall   | outdoor | 13 |
| Women's Track      | 55 | Moderate | both   | both    | 13 |
| Baseball           | 48 | Moderate | spring | outdoor | 14 |
| Men's Lacrosse     | 43 | Moderate | spring | outdoor | 17 |
| Men's Wrestling    | 40 | High     | both   | indoor  | 23 |
| Football           | 95 | High     | fall   | outdoor | 48 |

409  
 410 Number of students, contact level (as determined via standardized definitions in **Appendix**  
 411 **Table 3**), season, location, and number of COVID-19 cases per sports team. Teams with fewer  
 412 than 5 cases were labeled as "< 5" to minimize the risk of de-anonymity. Teams are sorted by  
 413 number of COVID-19 cases, then by contact level.

414 **Appendix Table 3**

415 Appendix Table 3. Sports contact level definitions.  
 416

| Contact level | Definition  | CMU teams  |
|---------------|---|--|
| Low           | Individual or small group sports where contact within six feet of other participants can be avoided. Sports that can be conducted with social distancing, consistent wearing of face coverings when within six feet of other people, or individually with no sharing of equipment or the ability to clean the equipment between use by competitors. | Cross country, cycling, golf, swimming, tennis, triathlon, volleyball (club) |



|          |   |  |
|----------|---|--|
| Moderate | Team sports that can be played with only incidental or intermittent close contact between participants. This category may also include sports that involve close, sustained contact, but with protective equipment in place that may reduce the likelihood of respiratory particle transmission between participants OR sports where social distancing is possible but that use equipment that can't be cleaned between participants. | Baseball, cheerleading, lacrosse, track, volleyball (sand, indoor) |
| High     | Team sports with frequent or sustained close contact (and in many cases, face-to-face contact) between participants and high probability that respiratory particles will be transmitted between participants.   | Basketball, football, soccer, wrestling                            |

417  
 418 Definitions of contact levels for sports teams. Sports teams were assigned a contact level of  
 419 low, medium, or high based on variables that affect transmission risk, including physical  
 420 proximity and the use of face coverings. Contact-level categories were created by synthesizing  
 421 risk profiles defined from the California Department of Health's "Outdoor and Indoor Youth and  
 422 Recreational Adult Sports" communication in April 2021 and the Colorado High School Activities  
 423 Association 2020-2021 sports risk profiles.

## 424 Appendix Table 4

425 Appendix Table 4. Chi-square analyses.

426

| Variable                             | Chi-Square Statistic (df) | P-value (Uncorrected)  |
|--------------------------------------|---------------------------|------------------------|
| Class years (Fall 2020)              | 95.67 (5)                 | $4.31 \times 10^{-19}$ |
| Class years (Spring 2021)            | 296.95 (5)                | $4.54 \times 10^{-62}$ |
| Sports contact level                 | 36.59 (2)                 | $1.13 \times 10^{-8}$  |
| Sports location (indoor vs. outdoor) | 1.60 (1)                  | 0.21                   |
| Sports season                        | 10.22 (2)                 | 0.006                  |
| Sports teams                         | 75.08 (25)                | $6.60 \times 10^{-7}$  |
| Residence halls                      | 31.30 (11)                | $9.87 \times 10^{-4}$  |

427  
 428 Results of Pearson's chi-squared test for categorical variables assessed for COVID-19 disease  
 429 risk. Test statistics, degrees of freedom, and uncorrected p-values are reported.

## 430 Appendix Table 5

431 Appendix Table 5. Published viral genomic data for clinical and environmental specimens

432

| Sequence Identifier (clinical) | Biosample Accession | GenBank Accession | GISAIID Identifier | SRA Accession |
|--------------------------------|---------------------|-------------------|--------------------|---------------|
| USA/CO-Broad-CMU_00017/2020    | SAMN17211059        | MW521521          | EPI_ISL_872745     | SRS8145178    |
| USA/CO-Broad-CMU_00039/2020    | SAMN17211081        | MW521525          | EPI_ISL_872749     | SRS8145099    |
| USA/CO-Broad-CMU_00043/2020    | SAMN17211085        | MW521526          | EPI_ISL_872750     | SRS8145173    |
| USA/CO-Broad-CMU_00051/2020    | SAMN17211093        | MW521527          | EPI_ISL_872751     | SRS8145098    |
| USA/CO-Broad-CMU_00054/2020    | SAMN17211096        | MW521528          | EPI_ISL_872752     | SRS8145097    |
| USA/CO-Broad-CMU_00060/2020    | SAMN17211102        | MW521529          | EPI_ISL_872753     | SRS8145065    |
| USA/CO-Broad-CMU_00062/2020    | SAMN17211104        | MW521530          | EPI_ISL_872754     | SRS8145064    |

|                                    |              |          |                 |            |
|------------------------------------|--------------|----------|-----------------|------------|
| USA/CO-Broad-CMU_00063/2020        | SAMN17211105 | MW521531 | EPI_ISL_872755  | SRS8145063 |
| USA/CO-Broad-CMU_00064/2020        | SAMN17211106 | MW521532 | EPI_ISL_872756  | SRS8145095 |
| USA/CO-Broad-CMU_00073/2020        | SAMN17211115 | MW521533 | EPI_ISL_872757  | SRS8145059 |
| USA/CO-Broad-CMU_00075/2020        | SAMN17211117 | MW521534 | EPI_ISL_872758  | SRS8145057 |
| USA/CO-Broad-CMU_00079/2020        | SAMN17211121 | MW521535 | EPI_ISL_872759  | SRS8145055 |
| USA/CO-Broad-CMU_00080/2020        | SAMN17211122 | MW521536 | EPI_ISL_872760  | SRS8145054 |
| USA/CO-Broad-CMU_00084/2020        | SAMN17211126 | MW521537 | EPI_ISL_872761  | SRS8145052 |
| USA/CO-Broad-CMU_00088/2020        | SAMN17211130 | MW521539 | EPI_ISL_872763  | SRS8145050 |
| USA/CO-Broad-CMU_00089/2020        | SAMN17211131 | MW521540 | EPI_ISL_872764  | SRS8145049 |
| USA/CO-Broad-CMU_00090/2020        | SAMN17211132 | MW521541 | EPI_ISL_872765  | SRS8145048 |
| USA/CO-Broad-CMU_00091/2020        | SAMN17211133 | MW521542 | EPI_ISL_872766  | SRS8145166 |
| USA/CO-Broad-CMU_00092/2020        | SAMN17211134 | MW521543 | EPI_ISL_872767  | SRS8145165 |
| USA/CO-Broad-CMU_00094/2020        | SAMN17211136 | MW521544 | EPI_ISL_872768  | SRS8145046 |
| USA/CO-Broad-CMU_00098/2020        | SAMN17211140 | MW521545 | EPI_ISL_872769  | SRS8145162 |
| USA/CO-Broad-CMU_00100/2020        | SAMN17211142 | MW521546 | EPI_ISL_872770  | SRS8145160 |
| USA/CO-Broad-CMU_00101/2020        | SAMN17211143 | MW521547 | EPI_ISL_872771  | SRS8145159 |
| USA/CO-Broad-CMU_00103/2020        | SAMN17211145 | MW521548 | EPI_ISL_872772  | SRS8145157 |
| USA/CO-Broad-CMU_00004/2020        | SAMN17210672 | MW454484 | EPI_ISL_765574  | pending    |
| USA/CO-Broad-CMU_00007/2020        | SAMN17210675 | MW454485 | EPI_ISL_765575  | pending    |
| USA/CO-Broad-CMU_00010/2020        | SAMN17210678 | MW454486 | EPI_ISL_765576  | pending    |
| USA/CO-Broad-CMU_00107/2020        | SAMN17211149 | MW521549 | EPI_ISL_872773  | SRS8145044 |
| USA/CO-Broad-CMU_00108/2020        | SAMN17211150 | MW521550 | EPI_ISL_872774  | SRS8145043 |
| USA/CO-Broad-CMU_00109/2020        | SAMN17211151 | MW521551 | EPI_ISL_872775  | SRS8145155 |
| USA/CO-Broad-CMU_00110/2020        | SAMN17211152 | MW521552 | EPI_ISL_872776  | SRS8145154 |
| USA/CO-Broad-CMU_00111/2020        | SAMN17211153 | MW521553 | EPI_ISL_872777  | SRS8145093 |
| USA/CO-Broad-CMU_00113/2020        | SAMN17211155 | MW454487 | EPI_ISL_765577  | pending    |
| USA/CO-Broad-CMU_00114/2020        | SAMN17211156 | MW454488 | EPI_ISL_765578  | pending    |
| USA/CO-Broad-CMU_00116/2020        | SAMN17211158 | MW454489 | EPI_ISL_765579  | pending    |
| USA/CO-Broad-CMU_00118/2020        | SAMN17211160 | MW454490 | EPI_ISL_765580  | pending    |
| USA/CO-Broad-CMU_00123/2020        | SAMN17211165 | MW454492 | EPI_ISL_765582  | pending    |
| USA/CO-Broad_WarriorLab-00125/2021 | SAMN17906199 | MW617630 | EPI_ISL_1011598 | SRS8270659 |
| USA/CO-Broad_WarriorLab-00126/2021 | SAMN17906200 | MW617631 | EPI_ISL_1011599 | SRS8270657 |
| USA/CO-Broad_WarriorLab-00128/2021 | SAMN17906202 | MW617632 | EPI_ISL_1011600 | SRS8270660 |
| USA/CO-Broad_WarriorLab-00130/2021 | SAMN17906204 | MW617633 | EPI_ISL_1011601 | SRS8270663 |
| USA/CO-Broad_WarriorLab-00131/2021 | SAMN17906205 | MW617634 | EPI_ISL_1011602 | SRS8270664 |
| USA/CO-Broad_WarriorLab-00132/2021 | SAMN17906206 | MW617635 | EPI_ISL_1011603 | SRS8270666 |
| USA/CO-Broad_WarriorLab-00133/2021 | SAMN17906207 | MW617636 | EPI_ISL_1011604 | SRS8270665 |
| USA/CO-Broad_WarriorLab-00134/2021 | SAMN17906208 | MW617637 | EPI_ISL_1011605 | SRS8270667 |
| USA/CO-Broad_WarriorLab-00135/2021 | SAMN17906209 | MW617638 | EPI_ISL_1011606 | SRS8270668 |
| USA/CO-Broad_WarriorLab-00136/2021 | SAMN17906210 | MW617639 | EPI_ISL_1011607 | SRS8270669 |
| USA/CO-Broad_WarriorLab-00137/2021 | SAMN17906211 | MW617640 | EPI_ISL_1011608 | SRS8270670 |
| USA/CO-Broad_WarriorLab-00138/2021 | SAMN17906212 | MW617641 | EPI_ISL_1011609 | SRS8270671 |
| USA/CO-Broad_WarriorLab-00140/2021 | SAMN17906214 | MW617642 | EPI_ISL_1011610 | SRS8270675 |
| USA/CO-Broad_WarriorLab-00141/2021 | SAMN17906215 | MW617643 | EPI_ISL_1011611 | SRS8270674 |
| USA/CO-Broad_WarriorLab-00142/2021 | SAMN17906216 | MW617644 | EPI_ISL_1011612 | SRS8270676 |
| USA/CO-Broad_WarriorLab-00145/2021 | SAMN17906219 | MW617645 | EPI_ISL_1011613 | SRS8270679 |
| USA/CO-Broad_WarriorLab-00146/2021 | SAMN17906220 | MW617646 | EPI_ISL_1011614 | SRS8270680 |
| USA/CO-Broad_WarriorLab-00147/2021 | SAMN17906221 | MW617647 | EPI_ISL_1011615 | SRS8270681 |
| USA/CO-Broad_WarriorLab-00148/2021 | SAMN17906222 | MW617648 | EPI_ISL_1011616 | SRS8270682 |
| USA/CO-Broad_WarriorLab-00187/2021 | SAMN17906261 | MW617679 | EPI_ISL_1011647 | SRS8270725 |
| USA/CO-Broad_WarriorLab-00188/2021 | SAMN17906262 | MW617680 | EPI_ISL_1011648 | SRS8270724 |
| USA/CO-Broad_WarriorLab-00189/2021 | SAMN17906263 | MW617681 | EPI_ISL_1011649 | SRS8270726 |
| USA/CO-Broad_WarriorLab-00190/2021 | SAMN17906264 | MW617682 | EPI_ISL_1011650 | SRS8270727 |
| USA/CO-Broad_WarriorLab-00191/2021 | SAMN17906265 | MW617683 | EPI_ISL_1011651 | SRS8270729 |
| USA/CO-Broad_WarriorLab-00192/2021 | SAMN17906266 | MW617684 | EPI_ISL_1011652 | SRS8270731 |
| USA/CO-Broad_WarriorLab-00162/2021 | SAMN17906236 | MW617658 | EPI_ISL_1011626 | SRS8270697 |
| USA/CO-Broad_WarriorLab-00177/2021 | SAMN17906251 | MW617670 | EPI_ISL_1011638 | SRS8270711 |
| USA/CO-Broad_WarriorLab-00178/2021 | SAMN17906252 | MW617671 | EPI_ISL_1011639 | SRS8270714 |
| USA/CO-Broad_WarriorLab-00182/2021 | SAMN17906256 | MW617674 | EPI_ISL_1011642 | SRS8270719 |
| USA/CO-Broad_WarriorLab-00149/2021 | SAMN17906223 | MW617649 | EPI_ISL_1011617 | SRS8270684 |
| USA/CO-Broad_WarriorLab-00150/2021 | SAMN17906224 | MW617650 | EPI_ISL_1011618 | SRS8270685 |
| USA/CO-Broad_WarriorLab-00151/2021 | SAMN17906225 | MW617651 | EPI_ISL_1011619 | SRS8270686 |

|                                    |              |          |                 |            |
|------------------------------------|--------------|----------|-----------------|------------|
| USA/CO-Broad_WarriorLab-00152/2021 | SAMN17906226 | MW617652 | EPI_ISL_1011620 | SRS8270687 |
| USA/CO-Broad_WarriorLab-00153/2021 | SAMN17906227 | MW617653 | EPI_ISL_1011621 | SRS8270688 |
| USA/CO-Broad_WarriorLab-00156/2021 | SAMN17906230 | MW617654 | EPI_ISL_1011622 | SRS8270691 |
| USA/CO-Broad_WarriorLab-00157/2021 | SAMN17906231 | MW617655 | EPI_ISL_1011623 | SRS8270689 |
| USA/CO-Broad_WarriorLab-00158/2021 | SAMN17906232 | MW617656 | EPI_ISL_1011624 | SRS8270692 |
| USA/CO-Broad_WarriorLab-00163/2021 | SAMN17906237 | MW617659 | EPI_ISL_1011627 | SRS8270698 |
| USA/CO-Broad_WarriorLab-00167/2021 | SAMN17906241 | MW617661 | EPI_ISL_1011629 | SRS8270701 |
| USA/CO-Broad_WarriorLab-00168/2021 | SAMN17906242 | MW617662 | EPI_ISL_1011630 | SRS8270703 |
| USA/CO-Broad_WarriorLab-00160/2021 | SAMN17906234 | MW617657 | EPI_ISL_1011625 | SRS8270695 |
| USA/CO-Broad_WarriorLab-00169/2021 | SAMN17906243 | MW617663 | EPI_ISL_1011631 | SRS8270702 |
| USA/CO-Broad_WarriorLab-00172/2021 | SAMN17906246 | MW617665 | EPI_ISL_1011633 | SRS8270708 |
| USA/CO-Broad_WarriorLab-00173/2021 | SAMN17906247 | MW617666 | EPI_ISL_1011634 | SRS8270709 |
| USA/CO-Broad_WarriorLab-00176/2021 | SAMN17906250 | MW617669 | EPI_ISL_1011637 | SRS8270713 |
| USA/CO-Broad_WarriorLab-00179/2021 | SAMN17906253 | MW617672 | EPI_ISL_1011640 | SRS8270715 |
| USA/CO-Broad_WarriorLab-00181/2021 | SAMN17906255 | MW617673 | EPI_ISL_1011641 | SRS8270717 |
| USA/CO-Broad_WarriorLab-00183/2021 | SAMN17906257 | MW617675 | EPI_ISL_1011643 | SRS8270720 |
| USA/CO-Broad_WarriorLab-00184/2021 | SAMN17906258 | MW617676 | EPI_ISL_1011644 | SRS8270722 |
| USA/CO-Broad_WarriorLab-00185/2021 | SAMN17906259 | MW617677 | EPI_ISL_1011645 | SRS8270721 |
| USA/CO-Broad_WarriorLab-00186/2021 | SAMN17906260 | MW617678 | EPI_ISL_1011646 | SRS8270723 |
| USA/CO-Broad_WarriorLab-00193/2021 | SAMN17906267 | MW617685 | EPI_ISL_1011653 | SRS8270730 |
| USA/CO-Broad_WarriorLab-00194/2021 | SAMN17906268 | MW617686 | EPI_ISL_1011654 | SRS8270732 |
| USA/CO-Broad_WarriorLab-00195/2021 | SAMN17906269 | MW617687 | EPI_ISL_1011655 | SRS8270733 |
| USA/CO-Broad_WarriorLab-00196/2021 | SAMN17906270 | MW617688 | EPI_ISL_1011656 | SRS8270734 |
| USA/CO-Broad_WarriorLab-00197/2021 | SAMN17906271 | MW617689 | EPI_ISL_1011657 | SRS8270735 |
| USA/CO-Broad_WarriorLab-00198/2021 | SAMN17906272 | MW617690 | EPI_ISL_1011658 | SRS8270736 |
| USA/CO-Broad_WarriorLab-00199/2021 | SAMN17906273 | MW617691 | EPI_ISL_1011659 | SRS8270737 |
| USA/CO-Broad_WarriorLab-00200/2021 | SAMN17906274 | MW617692 | EPI_ISL_1011660 | SRS8270739 |
| USA/CO-Broad_WarriorLab-00201/2021 | SAMN17906275 | MW617693 | EPI_ISL_1011661 | SRS8270740 |
| USA/CO-Broad_WarriorLab-00202/2021 | SAMN17906276 | MW617694 | EPI_ISL_1011662 | SRS8270741 |
| USA/CO-Broad_WarriorLab-00203/2021 | SAMN17906277 | MW617695 | EPI_ISL_1011663 | SRS8270742 |
| USA/CO-Broad_WarriorLab-00204/2021 | SAMN17906278 | MW617696 | EPI_ISL_1011664 | SRS8270744 |
| USA/CO-Broad_WarriorLab-00205/2021 | SAMN17906279 | MW617697 | EPI_ISL_1011665 | SRS8270743 |
| USA/CO-Broad_WarriorLab-00206/2021 | SAMN17906280 | MW617698 | EPI_ISL_1011666 | SRS8270745 |
| USA/CO-Broad_WarriorLab-00207/2021 | SAMN17906281 | MW617699 | EPI_ISL_1011667 | SRS8270746 |
| USA/CO-Broad_WarriorLab-00208/2021 | SAMN17906282 | MW617700 | EPI_ISL_1011668 | SRS8270747 |
| USA/CO-Broad_WarriorLab-00209/2021 | SAMN17906283 | MW617701 | EPI_ISL_1011669 | SRS8270748 |
| USA/CO-Broad_WarriorLab-00210/2021 | SAMN17906284 | MW617702 | EPI_ISL_1011670 | SRS8270749 |
| USA/CO-Broad_WarriorLab-00211/2021 | SAMN17906285 | MW617703 | EPI_ISL_1011671 | SRS8270750 |
| USA/CO-Broad_WarriorLab-00212/2021 | SAMN17906286 | MW617704 | EPI_ISL_1011672 | SRS8270752 |
| USA/CO-Broad_WarriorLab-00213/2021 | SAMN17906287 | MW617705 | EPI_ISL_1011673 | SRS8270753 |
| USA/CO-Broad_WarriorLab-00215/2021 | SAMN17906289 | MW617706 | EPI_ISL_1011674 | SRS8270754 |
| USA/CO-Broad_WarriorLab-00216/2021 | SAMN17906290 | MW617707 | EPI_ISL_1011675 | SRS8270755 |
| USA/CO-Broad_WarriorLab-00217/2021 | SAMN17906291 | MW617708 | EPI_ISL_1011676 | SRS8270756 |
| USA/CO-Broad_WarriorLab-00218/2021 | SAMN17906292 | MW617709 | EPI_ISL_1011677 | SRS8270758 |
| USA/CO-Broad_WarriorLab-00219/2021 | SAMN18306824 | MW749874 | EPI_ISL_1253885 | SRS8468532 |
| USA/CO-Broad_WarriorLab-00220/2021 | SAMN18306825 | MW749875 | EPI_ISL_1253886 | SRS8468533 |
| USA/CO-Broad_WarriorLab-00221/2021 | SAMN18306826 | MW749876 | EPI_ISL_1253887 | SRS8468534 |
| USA/CO-Broad_WarriorLab-00222/2021 | SAMN18306827 | MW749877 | EPI_ISL_1253888 | SRS8468535 |
| USA/CO-Broad_WarriorLab-00225/2021 | SAMN18306830 | MW749878 | EPI_ISL_1253889 | SRS8468539 |
| USA/CO-Broad_WarriorLab-00226/2021 | SAMN18306831 | MW749879 | EPI_ISL_1253890 | SRS8468540 |
| USA/CO-Broad_WarriorLab-00227/2021 | SAMN18306832 | MW749880 | EPI_ISL_1253891 | SRS8468541 |
| USA/CO-Broad_WarriorLab-00228/2021 | SAMN18306833 | MW749881 | EPI_ISL_1253892 | SRS8468542 |
| USA/CO-Broad_WarriorLab-00229/2021 | SAMN18306834 | MW749882 | EPI_ISL_1253893 | SRS8468543 |
| USA/CO-Broad_WarriorLab-00230/2021 | SAMN18306835 | MW749883 | EPI_ISL_1253894 | SRS8468544 |
| USA/CO-Broad_WarriorLab-00231/2021 | SAMN18306836 | MW749884 | EPI_ISL_1253895 | SRS8468545 |
| USA/CO-Broad_WarriorLab-00287/2021 | SAMN18306892 | MW749928 | EPI_ISL_1253939 | SRS8468340 |
| USA/CO-Broad_WarriorLab-00288/2021 | SAMN18306893 | MW749929 | EPI_ISL_1253940 | SRS8468257 |
| USA/CO-Broad_WarriorLab-00232/2021 | SAMN18306837 | MW749885 | EPI_ISL_1253896 | SRS8468546 |
| USA/CO-Broad_WarriorLab-00233/2021 | SAMN18306838 | MW749886 | EPI_ISL_1253897 | SRS8468547 |
| USA/CO-Broad_WarriorLab-00234/2021 | SAMN18306839 | MW749887 | EPI_ISL_1253898 | SRS8468548 |
| USA/CO-Broad_WarriorLab-00235/2021 | SAMN18306840 | MW749888 | EPI_ISL_1253899 | SRS8468551 |
| USA/CO-Broad_WarriorLab-00236/2021 | SAMN18306841 | MW749889 | EPI_ISL_1253900 | SRS8468552 |

|   |                            |                          |                          |                      |
|---|----------------------------|--------------------------|--------------------------|----------------------|
| USA/CO-Broad_WarriorLab-00237/2021      | SAMN18306842               | MW749890                 | EPI_ISL_1253901          | SRS8468386           |
| USA/CO-Broad_WarriorLab-00239/2021      | SAMN18306844               | MW749891                 | EPI_ISL_1253902          | SRS8468388           |
| USA/CO-Broad_WarriorLab-00241/2021      | SAMN18306846               | MW749892                 | EPI_ISL_1253903          | SRS8468390           |
| USA/CO-Broad_WarriorLab-00242/2021      | SAMN18306847               | MW749893                 | EPI_ISL_1253904          | SRS8468391           |
| USA/CO-Broad_WarriorLab-00243/2021      | SAMN18306848               | MW749894                 | EPI_ISL_1253905          | SRS8468392           |
| USA/CO-Broad_WarriorLab-00244/2021      | SAMN18306849               | MW749895                 | EPI_ISL_1253906          | SRS8468393           |
| USA/CO-Broad_WarriorLab-00245/2021      | SAMN18306850               | MW749896                 | EPI_ISL_1253907          | SRS8468395           |
| USA/CO-Broad_WarriorLab-00246/2021      | SAMN18306851               | MW749897                 | EPI_ISL_1253908          | SRS8468396           |
| USA/CO-Broad_WarriorLab-00248/2021      | SAMN18306853               | MW749898                 | EPI_ISL_1253909          | SRS8468398           |
| USA/CO-Broad_WarriorLab-00249/2021      | SAMN18306854               | MW749899                 | EPI_ISL_1253910          | SRS8468399           |
| USA/CO-Broad_WarriorLab-00250/2021      | SAMN18306855               | MW749900                 | EPI_ISL_1253911          | SRS8468400           |
| USA/CO-Broad_WarriorLab-00251/2021      | SAMN18306856               | MW749901                 | EPI_ISL_1253912          | SRS8468401           |
| USA/CO-Broad_WarriorLab-00252/2021      | SAMN18306857               | MW749902                 | EPI_ISL_1253913          | SRS8468402           |
| USA/CO-Broad_WarriorLab-00253/2021      | SAMN18306858               | MW749903                 | EPI_ISL_1253914          | SRS8468403           |
| USA/CO-Broad_WarriorLab-00256/2021      | SAMN18306861               | MW749904                 | EPI_ISL_1253915          | SRS8468407           |
| USA/CO-Broad_WarriorLab-00257/2021      | SAMN18306862               | MW749905                 | EPI_ISL_1253916          | SRS8468408           |
| USA/CO-Broad_WarriorLab-00258/2021      | SAMN18306863               | MW749906                 | EPI_ISL_1253917          | SRS8468409           |
| USA/CO-Broad_WarriorLab-00260/2021      | SAMN18306865               | MW749907                 | EPI_ISL_1253918          | SRS8468411           |
| USA/CO-Broad_WarriorLab-00261/2021      | SAMN18306866               | MW749908                 | EPI_ISL_1253919          | SRS8468412           |
| USA/CO-Broad_WarriorLab-00262/2021      | SAMN18306867               | MW749909                 | EPI_ISL_1253920          | SRS8468413           |
| USA/CO-Broad_WarriorLab-00263/2021      | SAMN18306868               | MW749910                 | EPI_ISL_1253921          | SRS8468313           |
| USA/CO-Broad_WarriorLab-00264/2021      | SAMN18306869               | MW749911                 | EPI_ISL_1253922          | SRS8468314           |
| USA/CO-Broad_WarriorLab-00265/2021      | SAMN18306870               | MW749912                 | EPI_ISL_1253923          | SRS8468316           |
| USA/CO-Broad_WarriorLab-00266/2021      | SAMN18306871               | MW749913                 | EPI_ISL_1253924          | SRS8468317           |
| USA/CO-Broad_WarriorLab-00267/2021      | SAMN18306872               | MW749914                 | EPI_ISL_1253925          | SRS8468318           |
| USA/CO-Broad_WarriorLab-00268/2021      | SAMN18306873               | MW749915                 | EPI_ISL_1253926          | SRS8468319           |
| USA/CO-Broad_WarriorLab-00269/2021      | SAMN18306874               | MW749916                 | EPI_ISL_1253927          | SRS8468320           |
| USA/CO-Broad_WarriorLab-00271/2021      | SAMN18306876               | MW749917                 | EPI_ISL_1253928          | SRS8468322           |
| USA/CO-Broad_WarriorLab-00272/2021      | SAMN18306877               | MW749918                 | EPI_ISL_1253929          | SRS8468323           |
| USA/CO-Broad_WarriorLab-00273/2021      | SAMN18306878               | MW749919                 | EPI_ISL_1253930          | SRS8468324           |
| USA/CO-Broad_WarriorLab-00275/2021      | SAMN18306880               | MW749920                 | EPI_ISL_1253931          | SRS8468327           |
| USA/CO-Broad_WarriorLab-00282/2021      | SAMN18306887               | MW749923                 | EPI_ISL_1253934          | SRS8468334           |
| USA/CO-Broad_WarriorLab-00276/2021      | SAMN18306881               | MW749921                 | EPI_ISL_1253932          | SRS8468328           |
| USA/CO-Broad_WarriorLab-00278/2021      | SAMN18306883               | MW749922                 | EPI_ISL_1253933          | SRS8468330           |
| USA/CO-Broad_WarriorLab-00283/2021      | SAMN18306888               | MW749924                 | EPI_ISL_1253935          | SRS8468335           |
| USA/CO-Broad_WarriorLab-00284/2021      | SAMN18306889               | MW749925                 | EPI_ISL_1253936          | SRS8468336           |
| USA/CO-Broad_WarriorLab-00285/2021      | SAMN18306890               | MW749926                 | EPI_ISL_1253937          | SRS8468338           |
| USA/CO-Broad_WarriorLab-00286/2021      | SAMN18306891               | MW749927                 | EPI_ISL_1253938          | SRS8468339           |
| USA/CO-CDCBI-Warrior_00289/2021         | SAMN18498486               | MW834877                 | EPI_ISL_1413769          | SRS8613058           |
| USA/CO-CDCBI-Warrior_00290/2021         | SAMN18498487               | MW834878                 | EPI_ISL_1413771          | SRS8613060           |
| USA/CO-CDCBI-Warrior_00291/2021         | SAMN18498488               | MW834879                 | EPI_ISL_1413774          | SRS8613059           |
| USA/CO-CDCBI-Warrior_00292/2021         | SAMN18498489               | MW834880                 | EPI_ISL_1413776          | SRS8613061           |
| USA/CO-CDCBI-Warrior_00293/2021         | SAMN18498490               | MW834881                 | EPI_ISL_1413779          | SRS8613063           |
| USA/CO-CDCBI-Warrior_00294/2021         | SAMN18498491               | MW834882                 | EPI_ISL_1413781          | SRS8613064           |
| USA/CO-CDCBI-Warrior_00295/2021         | SAMN18498492               | MW834883                 | EPI_ISL_1413784          | SRS8613065           |
| USA/CO-CDCBI-Warrior_00296/2021         | SAMN18498493               | MW834884                 | EPI_ISL_1413787          | SRS8613066           |
| USA/CO-CDCBI-Warrior_00300/2021         | SAMN18790465               | MZ217780                 | EPI_ISL_2133621          | SRS8763083           |
| USA/CO-CDCBI-Warrior_00301/2021         | SAMN18790466               | MZ217781                 | EPI_ISL_2133623          | SRS8763082           |
| USA/CO-CDCBI-Warrior_00302/2021         | SAMN18790467               | MZ217782                 | EPI_ISL_2133625          | SRS8763084           |
| USA/CO-CDCBI-Warrior_00304/2021         | SAMN18790469               | MZ217783                 | EPI_ISL_2133626          | SRS8763087           |
| USA/CO-CDCBI-Warrior_00305/2021         | SAMN18790470               | MZ217784                 | EPI_ISL_2133628          | SRS8763088           |
| USA/CO-CDCBI-Warrior_00312/2021         | SAMN19224119               | MZ217786                 | EPI_ISL_2133928          | SRS9003810           |
| USA/CO-CDCBI-Warrior_00311/2021         | SAMN19224118               | MZ217785                 | EPI_ISL_2133927          | SRS9003809           |
| <b>Sequence Identifier (wastewater)</b> | <b>Biosample Accession</b> | <b>GenBank Accession</b> | <b>GISAID Identifier</b> | <b>SRA Accession</b> |
| USA-CO-Broad_CMU_W0011-2021             | SAMN29048169               |                          |                          | SRR19659512          |
| USA-CO-Broad_CMU_W0012-2021             | SAMN29048170               |                          |                          | SRR19659511          |
| USA-CO-Broad_CMU_W0013-2021             | SAMN29048171               |                          |                          | SRR19659500          |
| USA-CO-Broad_CMU_W0014-2021             | SAMN29048172               |                          |                          | SRR19659489          |
| USA-CO-Broad_CMU_W0015-2021             | SAMN29048173               |                          |                          | SRR19659478          |
| USA-CO-Broad_CMU_W0016-2021             | SAMN29048174               |                          |                          | SRR19659475          |
| USA-CO-Broad_CMU_W0017-2021             | SAMN29048175               |                          |                          | SRR19659474          |



|              |      |         |      |  |      |      |      |      |      |      |
|--------------|------|---------|------|--|------|------|------|------|------|------|
| CO_CMU_W0017 | 2-17 | Site 6  |      |  | 0.91 |      |      |      |      |      |
| CO_CMU_W0018 | 2-17 | Site 7  |      |  | 1.00 |      |      |      |      |      |
| CO_CMU_W0019 | 2-17 | Site 11 |      |  |      |      |      |      |      |      |
| CO_CMU_W0020 | 2-17 | Site 4  |      |  |      |      |      |      | 1.00 |      |
| CO_CMU_W0021 | 2-17 | Site 2  |      |  | 0.93 |      |      |      |      |      |
| CO_CMU_W0030 | 2-11 | Site 6  |      |  | 0.13 | 0.31 |      |      | 0.54 |      |
| CO_CMU_W0034 | 2-15 | Site 5  |      |  | 0.28 |      |      |      | 0.47 |      |
| CO_CMU_W0040 | 2-18 | Site 11 |      |  | 0.79 |      |      |      |      |      |
| CO_CMU_W0043 | 2-18 | Site 8  |      |  |      |      |      | 0.16 | 0.81 |      |
| CO_CMU_W0082 | 3-01 | Site 6  |      |  |      |      |      |      | 0.93 |      |
| CO_CMU_W0084 | 3-01 | Site 4  |      |  | 0.99 |      |      |      |      |      |
| CO_CMU_W0094 | 3-04 | Site 5  |      |  | 0.58 |      |      |      | 0.34 |      |
| CO_CMU_W0095 | 3-04 | Site 3  |      |  | 0.49 |      |      |      | 0.26 |      |
| CO_CMU_W0109 | 3-09 | Site 1  |      |  |      |      |      |      | 1.00 |      |
| CO_CMU_W0130 | 3-18 | Site 1  |      |  |      |      |      |      | 0.31 |      |
| CO_CMU_W0031 | 2-11 | Site 1  |      |  |      |      | 0.03 |      | 0.96 |      |
| CO_CMU_W0033 | 2-15 | Site 10 |      |  |      |      |      |      | 0.99 |      |
| CO_CMU_W0035 | 2-18 | Site 5  |      |  | 0.99 |      |      |      |      |      |
| CO_CMU_W0038 | 2-18 | Site 4  |      |  | 0.99 |      |      |      |      |      |
| CO_CMU_W0039 | 2-18 | Site 1  |      |  | 0.93 |      |      |      | 0.05 |      |
| CO_CMU_W0042 | 2-18 | Site 10 |      |  |      |      |      |      | 0.99 |      |
| CO_CMU_W0046 | 2-22 | Site 4  |      |  | 0.99 |      |      |      |      |      |
| CO_CMU_W0058 | 2-23 | Site 11 |      |  | 0.98 |      |      |      |      |      |
| CO_CMU_W0059 | 2-23 | Site 5  |      |  |      |      |      |      | 0.85 |      |
| CO_CMU_W0062 | 2-23 | Site 1  |      |  |      |      |      |      | 1.00 |      |
| CO_CMU_W0069 | 2-25 | Site 5  |      |  | 0.99 |      |      |      |      |      |
| CO_CMU_W0070 | 2-25 | Site 3  |      |  |      |      |      |      | 0.96 |      |
| CO_CMU_W0101 | 3-08 | Site 3  |      |  |      |      |      |      | 0.99 |      |
| CO_CMU_W0107 | 3-08 | Site 5  |      |  |      |      |      |      | 0.94 |      |
| CO_CMU_W0108 | 3-09 | Site 3  |      |  |      |      |      |      | 0.99 |      |
| CO_CMU_W0127 | 3-16 | Site 5  | 0.12 |  | 0.08 |      |      |      | 0.72 | 0.07 |

439

440 Wastewater-detected lineages and their relative abundances. For each wastewater sample,  
 441 collection date and site of collection are also listed. Lineages and abundances were determined  
 442 via application of the Freyja program, as described in detail in the Supplementary Methods.

## 443 Appendix Table 7

444 Appendix Table 7. Replicate-confirmed single nucleotide variant mutations identified in  
 445 sequenced wastewater samples but not present in sequenced clinical samples

446

| SNV     | In CO | Change     | Gene   | Amino acid | Presence in proportion of 42 wastewater samples | Maximum allele frequency |
|---------|-------|------------|--------|------------|---|--------------------------|
| T5260A  | False | Synonymous | ORF1ab | T1665T     | 10%   | 29%                      |
| T6174G  | False | Missense   | ORF1ab | I1970S     | 17%   | 32%                      |
| T9843A  | False | Stop       | ORF1ab | L3193*     | 14%   | 4%                       |
| C10650T | False | Missense   | ORF1ab | T3462I     | 31%   | 100%                     |
| T27444G | False | Synonymous | ORF7a  | L17L       | 7%  | 27%                      |
| C835T   | True  | Synonymous | ORF1ab | F190F      | 38%   | 100%                     |
| C6501T  | True  | Missense   | ORF1ab | P2079L     | 38%   | 99%                      |
| G14126A | True  | Missense   | ORF1ab | S4621N     | 5%  | 100%                     |
| C21952T | True  | Synonymous | S      | V130V      | 38%   | 100%                     |
| T26099C | True  | Missense   | ORF3a  | I236T      | 33%   | 100%                     |
| C28344T | True  | Missense   | N      | T24I       | 38%   | 96%                      |

447

448 Replicate-confirmed mutations identified in wastewater samples from CMU, but not in clinical  
 449 samples. SNV nucleotide changes and positions are listed in bp, relative to the reference  
 450 ancestral genome, NC\_045512.2 (1st column) along with corresponding amino acid changes  
 451 (4th and 5th columns), the class of change (3rd column), the proportion of samples bearing the  
 452 change (6th column), and the highest allele frequency of that change amongst those samples  
 453 (final column). Some of these mutations were present in Colorado clinical viral genomes (2nd  
 454 column), or representative of specific Pango lineages (penultimate column).

## 455 Appendix Table 8

456 Appendix Table 8. Nucleotide and amino acid substitutions present in the B.1.429.1 lineage

457

| Region | Amino Acid Changes Characteristic of B.1.429 | Additional Amino Acid Changes Characteristic of B.1.429.1 |
|--------|--|---|
| ORF1a  | T265I, I4205V                                | F2827L, V3367I  |
| ORF1b  | P314L, D1183Y                                | P314L, D1183Y   |
| S      | S13I, W152C*, L452R*, D614G*                 | Q677H   |

|       |        |               |
|-------|--------|---------------|
| ORF3a | Q57H   | A23V          |
| N     | T205I* | P142S, M234I* |
| ORF8  |        | V100L         |

458  
 459 Characteristic amino acid mutations for B.1.429.1 and parent lineage B.1.429. Mutations are  
 460 categorized by location / gene. Mutations with an accompanying asterisk were not seen in all  
 461 B.1.429.1 sequenced genomes; however, this may have been due to gaps in sequencing  
 462 coverage.

### 463 Appendix Table 9

464 Appendix Table 9. Summary of data sources used at Colorado Mesa University for their  
 465 infectious disease surveillance program and additional recommendations for future institutional  
 466 surveillance programs.

467

|                                       | <b>Epidemiological Analyses</b>  | <b>Clinical Viral Genomic Sequencing</b>                             | <b>Wastewater Surveillance &amp; Sequencing</b>   | <b>Wifi Proximity Analyses</b>                       |
|---------------------------------------|--|--|---|--|
| <b>General Utility</b>                | Identify epidemiological risk factors  | Parametrize cluster distribution and identify lineages and mutations | Establish quality control standards   | Discriminate interaction patterns by test positivity |
| <b>Current Utility to Institution</b> | Specify athletic, residential, and class-year risks  | Identify VoC/VoI & transmission clusters                             | Designate testing resources based on surveillance; sequencing to detect mutations not seen clinically | _____  |
| <b>Potential for Future Utility</b>   | Automatically integrate metadata, wastewater surveillance, sequencing, and wifi-based contact tracing into comprehensive surveillance system made directly accessible for the community or public health officials |  |   |  |
| <b>Cost of Acquisition</b>            | <i>Medium:</i><br>Personnel (cataloging information)   | <i>Medium:</i><br>Transportation of excess clinical samples          | <i>Medium–High:</i><br>Establishment of collection devices  | <i>Low:</i><br>Established infrastructure            |
| <b>Cost of Analysis</b>               | <i>Low:</i> Personnel (analysis)   | <i>High:</i><br>Sequencing reagents and computing resources          | <i>Low:</i> PCR reagents  | <i>Low:</i><br>Computing resources                   |
|                                       |  |  | <i>Medium:</i><br>Sequencing costs reduced relative to clinical due to fewer samples                  |  |
| <b>Difficulty of Analysis</b>         | <i>Low:</i><br>Established statistical methods   | <i>Low:</i><br>Established tools for phylogenetic trees              | <i>Low:</i><br>Established tools for PCR analysis   | <i>High:</i><br>Few established tools                |



|  |  |  |  |  |
|--|--|--|--|--|
|  |  |  | <i>Medium:</i><br>Few established tools/methods<br>for mixed sequence analysis |  |
|--|--|--|--|--|

468  
469 Comparison of the utility and costs of each data source utilized in this study. We recommend  
470 incorporation of these tools in a specific manner given resource availability (Figure 7). VoC =  
471 Variant of Concern; VOI = Variant of Interest.

## 472 Appendix Table 10

473 Appendix Table 10. Jaccard similarity between clusters derived from genomic reconstruction  
474 supplemented by different contact tracing data sets

| Comparison Groups          | Cluster Color | Jaccard Similarity |
|----------------------------|---------------|--------------------|
| CT vs. 2-Day Wifi          | Orange        | .421               |
|                            | Light Blue    | 1.0                |
|                            | Pink          | 0.0                |
|                            | Yellow        | 1.0                |
| CT vs. 10-Day Wifi         | Orange        | .889               |
|                            | Light Blue    | 1.0                |
|                            | Pink          | 1.0                |
|                            | Yellow        | 1.0                |
| 2-Day Wifi vs. 10-Day Wifi | Orange        | .474               |
|                            | Light Blue    | 1.0                |
|                            | Pink          | 0                  |
|                            | Yellow        | 1.0                |

475  
476 We computed the Jaccard similarity for distinct transmission reconstruction networks for  
477 individuals with the B.1.429.1 lineage. We supplemented the genomic reconstruction in the trials  
478 using three different definitions of close contacts: (1) manual contact tracing data, (2) 10-day  
479 wifi-derived contacts, and (3) 2-day wifi-derived contacts.

## 480 Appendix Table 11

481 Appendix Table 11. Summary of metrics used for the wifi proximity network analyses

482

| Metric Name | Variables | Formula and Text Description | Figure Panel |
|-------------|-----------|------------------------------|--------------|
|-------------|-----------|------------------------------|--------------|

|  |                                       |  |   |
|--|---------------------------------------|--|---|
| <b>(Median of) Daily Contacts</b>                    | <i>individual</i>                     | $\text{Median} \left\{ \begin{array}{l} \text{for each day present on campus:} \\ \text{number of unique contacts for } \textit{individual} \end{array} \right\}$ <p>For each day that an individual is present on campus, calculate number of unique contacts; then take the median.</p>  | Figure 3A, left                         |
| <b>(Median of) Average Exposure Time per Contact</b> | <i>individual</i>                     | $\text{Median} \left\{ \frac{\sum_{\text{unique contacts}} \text{total interaction time with } \textit{individual}}{\text{number of unique contacts for } \textit{individual}} \right\}$ <p>For each day that an individual is present on campus, calculate the total time spent with all contacts and the number of unique contacts. Divide the total time by the number of contacts per day and take the median of these values.</p>   | Figure 3A, right                        |
| <b>Number of Days on Campus</b>                      | <i>individual</i>                     | <p># of days that <i>individual</i> is connected to an AP</p> <p>Calculate the number of days an individual is present on campus.</p>  | Appendix Figure 5AB; Appendix Figure 7B |
| <b>Number of Individuals on Campus</b>               | <i>day, user category</i>             | <p># of individuals of <i>user category</i> connected to an AP on <i>day</i></p> <p>For a given day, calculate the number of unique individuals of a given user category (i.e. semester positive vs semester negative) that are present on campus.</p>   | Appendix Figure 5CD, left               |
| <b>Proportion of Individuals on Campus</b>           | <i>day, user category</i>             | $\frac{\text{\# of individuals of } \textit{user category} \text{ connected to an AP on } \textit{day}}{\text{Max} \left\{ \begin{array}{l} \text{for each day:} \\ \text{\# of individuals of } \textit{user category} \text{ connected to an AP} \end{array} \right\}}$ <p>For a given day, calculate the number of users of a given user category (i.e., semester positive or semester negative) present on campus. Divide by the maximum value of this metric for the given user category across all days.</p> | Appendix Figure 5CD, right              |
| <b>(Median of) Median Duration of AP Connections</b> | <i>day of week, building category</i> | $\text{Median} \left\{ \text{Median} \left\{ \begin{array}{l} \text{for each day } \in \textit{day of week:} \\ \text{for each AP connection } \in \textit{building category:} \\ \text{duration of connection} \end{array} \right\} \right\}$ <p>For a given building type and a given day of the week (i.e., Monday), calculate the median AP connection duration for each day; then take the median. Building type can be 'all', 'residential', 'other', or 'academic'.</p>                                     | Appendix Figure 6AB                     |
| <b>(Median of) Daily Number of AP Connections</b>    | <i>day of week, building category</i> | $\text{Median} \left\{ \begin{array}{l} \text{for each day } \in \textit{day of week:} \\ \text{\#number of AP connections } \in \textit{building category} \end{array} \right\}$ <p>For a given building type and a given day of the week (i.e., Monday), calculate the total number of AP connections for each day; then take the median. Building type can be 'all', 'residential', 'other', or 'academic'.</p>   | Appendix Figure 6CD                     |
| <b>Total Daily Interaction Duration</b>              | <i>pair, day</i>                      | $\sum_{\text{all interactions of } \textit{pair} \text{ on } \textit{day}} \text{interaction duration}$  | Appendix Figure 7C; Appendix Figure 12A |

|  |                  |  |   |
|--|------------------|--|---|
|  |                  | Across all interactions for a given pair on a given day, calculate the total contact time between the pair. Pairs are defined as two individuals connecting to the same access point at the same time.   |   |
| <b>Median Daily Interaction Duration</b> | <i>pair, day</i> | $Median \left\{ \begin{array}{l} \text{for each interaction of } pair \text{ on } day: \\ \text{interaction duration} \end{array} \right\}$ <p>Across all interactions for a given pair on a given day, calculate the median contact time between the pair. Pairs are defined as two individuals connecting to the same access point at the same time.</p> | Appendix Figure 7D; Appendix Figure 12B |

483  
 484 The metric names, associated variables, formulas, text descriptions, and the associated figure  
 485 panel are listed for all metrics used in wifi proximity network analyses.